2008-01-01

Does Wind Affect Genetic Structure and Gene Flow in Two Phyllostomid Bat Species (Erophylla sezekorni and Macrotus waterhousii) in the Bahamas and Greater Antilles?

Robert Muscarella
University of Miami, bob.muscarella@gmail.com

UNIVERSITY OF MIAMI

DOES WIND AFFECT GENETIC STRUCTURE AND GENE FLOW IN TWO PHYLLOSTOMID BAT SPECIES (*Erophylla sezekorni* AND *Macrotus waterhousii*) IN THE BAHAMAS AND GREATER ANTILLES?

By

Robert Muscarella

A THESIS

Submitted to the Faculty
of the University of Miami
in partial fulfillment of the requirements for
the degree of Master of Science

Coral Gables, Florida

May 2008

UNIVERSITY OF MIAMI

A thesis submitted in partial fulfillment of
the requirements for the degree of
Master of Science

DOES WIND AFFECT GENETIC STRUCTURE AND GENE FLOW IN TWO PHYLLOSTOMID BAT SPECIES (*Erophylla sezekorni* AND *Macrotus waterhousii*) IN THE BAHAMAS AND GREATER ANTILLES?

Robert Muscarella

Approved:

Dr. Theodore H. Fleming Professor of Biology	Dr. Terri A. Scandura Dean of the Graduate School
Dr. Leonel da Silveira Lobo Sternberg Professor of Biology	Dr. Rinku Roy Chowdhury Assistant Professor of Geography
Dr. Alex C. Wilson Assistant Professor of Biology	

MUSCARELLA, ROBERT (M.S. Biology)
Does wind affect genetic structure and gene flow in two phyllostomid bat species (*Erophylla sezekorni* and *Macrotus waterhousii*) in the Bahamas and Greater Antilles? (May 2008)

Abstract of a thesis at the University of Miami.

Thesis supervised by Professor Theodore H. Fleming.
No. of pages in the text. (49)

Gene flow dictates a broad range of ecological and evolutionary processes. Understanding the factors mediating magnitude and direction of gene flow is crucial for interpreting patterns of genetic diversity and for answering many kinds of biological questions. Recent advances at the interface of population genetics and GIS technology have expanded our perspective of the geographic and physical features influencing gene flow and, in turn, shaping genetic structure of populations.

I investigated the effect of surface-level trade winds on genetic structure and gene flow in two species of phyllostomid bats in the Bahamas and Greater Antilles: *Erophylla sezekorni* (the buffy flower bat) and *Macrotus waterhousii* (Waterhouse's leaf-nosed bat). Bayesian Clustering Analysis revealed that all islands sampled represent independent genetic populations for *M. waterhousii* but not for *E. sezekorni*. Samples from 13 islands (spanning *E. sezekorni*'s range) clustered into five genetic populations and revealed the existence of two main clades (eastern: Hispaniola and Puerto Rico; western: Cuba, Jamaica, and Bahamas). To test the hypothesis that surface-level trade winds mediate gene flow in this system, I generated measures of effective distance between islands using anisotropic cost modeling based on wind data from the National Climactic Data Center. Both species exhibited significant isolation by distance with geographical distance and some of the measures of effective distance, but effective distance did not

provide increased explanatory power in predicting distribution of genetic diversity. The IBD_{GEO} slope was steeper for *E. sezekorni* than *M. waterhousii*, suggesting greater dispersal ability in the former species. According to Maximum Likelihood analysis, a majority (80%) of gene flow between genetic populations was asymmetric in both species. The degree of asymmetric gene flow between populations was not explained by the degree of asymmetry in effective distance or island area, indicating an unknown mechanism driving asymmetric gene flow. More information about the ecology of these taxa is required to understand the incidence of asymmetric gene flow in this system.

The results of this study suggest that gene flow among islands is highly restricted for *M. waterhousii* and that this species deserves greater taxonomic attention and conservation concern.

To all the lonely bats who have lost their mothers.

ACKNOWLEDGEMENTS

This thesis represents a collaborative project that would not have been possible without the guidance and participation of many people. First, I thank my committee, Drs. T. H. Fleming (committee chairperson), L. Sternberg, A. C. Wilson and R. R. Chowdhury. Ted Fleming continuously encouraged perseverance through the inevitable frustrations associated with research. Ultimately, his guidance helped me to understand that bumpy roads are part of scientific discovery. Leo Sternberg reminded me that studying life remains interesting only if you maintain your own. Alex Wilson exposed me to the wonder of molecular techniques as well as being an incredible source of friendship, support and encouragement. Rinku Roy Chowdhury helped tremendously with conceptual design, GIS advice and friendly support.

The graduate students in the Department of Biology have been a great source of help and inspiration. Specifically, Kevin Murray deserves much of the credit for this project. He performed the bulk of the fieldwork and lab work to generate the data used in this project. He also offered insightful suggestions. The wind data was obtained and processed by Derek Ortt, a graduate student at RSMAS. Besides providing friendly support, Nathan Muchhala, Summer Scobell, Christina McCain and Kate Semon helped tremendously with the conceptual design, methodological concerns and interpretation.

Numerous other people generously shared time and advice on technical and conceptual issues. Dr. Matthew Potts helped with statistics. Dr. Donald Olson helped with the conceptual design. Dr. Maria Villanueva provided the map of the study area.

Chris Hanson and Dr. S. S. Roy provided assistance with GIS software and data formatting issues. Dr. Peter Beerli (Florida State University) provided valuable advice and comments on the use of MIGRATE. Tissue samples were also donated or collected by C. A. Mancina (Cuba), C. McCain (Puerto Rico), L. G. Herrera (Mexico), A. Tejedor (Dominican Republic), L. M. Davalos and loan from American Museum of Natural History (Jamaica), R. J. Baker and loan from National Science Research Laboratory at the Museum of Texas Tech University (Jamaica and Cuba).

Finally, I would like to thank my family and friends who, by their diverse interests and opinions have contributed immensely to my scientific curiosity.

TABLE OF CONTENTS

LIST OF FIGURES

LIST OF TABLES

Chapter 1: Introduction

Gene flow dictates a broad range of ecological and evolutionary processes (Wright 1951; Slatkin 1987; Freeland 2005). Understanding the factors mediating the magnitude and direction of gene flow is crucial for interpreting patterns of genetic diversity and for answering many kinds of biological questions. Limitations associated with addressing the effects of large-scale, spatially dynamic variables have historically constrained our understanding of the influence of these processes on gene flow. Our ability to interpret spatial partitioning of genetic variation has consequently been restricted. Advances at the interface of population genetics and GIS technology have relaxed some of these limitations by expanding our perspective of the geographic and physical features influencing gene flow and, in turn, shaping genetic structure of populations (e.g. Coulon *et al.* 2004; Cushman *et al.* 2006; Vignieri 2005).

The emerging field of landscape genetics (Manel *et al.* 2003) deals explicitly with identifying genetic patterns and attributing them to landscape properties. For example, dispersal limitation theoretically leads to a positive relationship between Euclidean distance and genetic differentiation; this is the classic pattern of isolation by distance (IBD) (Wright 1946). Many studies have used straight-line Euclidean distance when investigating IBD patterns, relying on the tenuous assumption that the cost of movement across the landscape is uniform. A biologically meaningful measure of distance, however, must incorporate the response of the study organism to the physical forces and geographic features to which it is subject. Furthermore, various organisms may experience the effects of these factors in very different ways. In these regards, traditional distance metrics may inadequately describe biological reality. In an attempt to address

these shortcomings, researchers have recently begun incorporating GIS data of landscape variables with knowledge of the study organism's dispersal ability, habitat preferences, or other pertinent ecological information into genetic studies. These studies have converted measures of Euclidean distance into relative measures of 'effective distance' or 'functional connectivity' in order to predict spatial patterns of genetic variation with greater accuracy and precision (*e.g.* Funk *et al.* 2005; Spear *et al.* 2005; Stevens *et al.* 2005).

Studies exploring the concept of effective distance often implement 'least-cost' approaches whereby various habitat types are assigned relative values denoting known or assumed costs of movement to the organism. GIS technology is then used to find the route of least cumulative cost between sample sites or populations resulting in a relative measure of effective distance (e.g. Coulon *et al.* 2004; Vignieri 2005). Prior information on habitat preferences and dispersal ability is essential for constructing biologically realistic cost surfaces of this type (see Cushman *et al.* 2006 for a comprehensive approach). The vast majority of these studies have dealt with systems where costs to movement are isotropic. In other words, an organism traveling between two points on a landscape is assumed to face equivalent cost to movement in either direction. This may be a valid assumption in cases where topographic features or different habitat types impose differential costs to movement.

Directional (anisotropic) forces can also have dramatic effects on the movement of both passively and actively dispersing organisms (and their genes) through space. Theoretical work has shown that asymmetric gene flow can have profound consequences for evolutionary processes, metapopulation dynamics, biogeographical inference and the

design of effective conservation strategies (Thompson 1994; Telschow *et al.* 2006; Kawecki and Holt 2002; Cook and Crisp 2005; Vuilleumier and Possingham 2006). Evolutionary implications of asymmetric gene flow include the ability of populations to adapt to local conditions (Dias 1996) and the evolution of species' ranges (Kirkpatrick and Barton 1997). In spite of this, much theoretical and empirical work has been based on the assumption of symmetric gene flow (Hanski 1999; Whitlock and McCauley 1999).

The role of anisotropic forces in mediating gene flow is perhaps most immediately evident for anemochorous (wind-pollinated or-dispersed) plants. Few studies, however, have rigorously quantified wind patterns in an effort to explain genetic structure of anemochorous plant populations. In a review of air and sea current dispersal of plants across the tropical Atlantic, Renner (2004) inferred a role for wind using extremely generalized currents. Dutech *et al.* (2005) provided a more rigorous analysis of wind patterns in their study of wind-mediated pollen dispersal in a population of California Valley oaks. The authors attributed their finding no significant anisotropic effect of wind to the presumably non-directional diluting effect of seed dispersal on any potential directional genetic signal. In a broad scale study, Munoz *et al.* (2004) used anisotropic cost modeling with newly available data on global winds to show that wind-mediated dispersal of propagules explained the strong similarity of cryptogam floras among distant landmasses in the southern Hemisphere.

An analogous situation can be found in the role of water currents in shaping the dispersal kernels of many aquatic organisms during the pelagic portion of their life cycles. The resulting recruitment patterns can have broad implications for ecology and evolution of aquatic communities. For example, Galindo *et al.* (2006) used data on ocean

currents to develop a coupled oceanographic-genetic model that predicted genetic structure of Caribbean corals. In a study comparing genetic structure of benthic marine species, Wares *et al.* (2001) showed that ocean currents mediated asymmetric gene flow and genetic structure of species with a planktonic larval stage, but not for a species with nondispersing larvae. Hare *et al.* (2005) found that ocean current-mediated dispersal increased the steepness of clinal variation across species' ranges – a surprising result given the broad scale gene flow expected from marine larvae. Michels *et al.* (2001) made a 'plea' to include GIS cost modeling in isolation by distance studies because of their success in improving accuracy of gene flow estimates among zooplankton populations connected by directional overflows.

Despite these important contributions, there remains an overall paucity of empirical data on the particular mechanisms leading to asymmetric gene flow between populations as well as its overall incidence in nature, especially for actively dispersing organisms. In part, this results from the scarcity of proposed methodological approaches (Kennington *et al.* 2003). The complexity and variability of wind and water currents introduces further conceptual and analytical challenges. Fraser *et al.* (2004) found asymmetric gene flow in brook Charr (*Salvelinus fontinalis*), but the directional bias was primarily attributed to demographic differences (i.e. population sizes) rather than anisotropic forces. Telschow *et al.* (2006) showed that distorted sex ratios may also cause asymmetric gene flow independent of anisotropic forces. In contrast, Hanfling and Weetman (2006) were able to show that water currents mediated downstream asymmetric gene flow in a fish. Calsbeek and Smith (2003) found that island populations of *Anolis* lizards in the Bahamas were connected by directional gene flow mediated by ocean

currents. These latter two studies exemplify the great potential for incorporating anisotropic landscape forces in studies on gene flow in actively dispersing organisms.

The foraging, dispersal and migratory movements of volant animals can be especially strongly affected by wind (Liechti 2006; Akesson and Hedenstrom 2007; Shamoun-Baranes *et al.* 2007). Perhaps most importantly, energetic constraints to travel can theoretically result in a directional bias in the movement of individuals resulting in asymmetric gene flow among populations. Generally, the range of directions potentially traveled by a flying animal (the 'scope of orientation') will be determined by the relationship between the wind speed and the airspeed of the animal relative to the surrounding air. In a simplified description provided by Akesson and Hedenstrom (2007), the scope of orientation is unrestricted when the wind speed is less than the airspeed; the scope is limited to 180° when the two speeds are equal; and the scope of orientation decreases as the wind speed gets progressively greater than the animal's airspeed. In sum, wind is likely to dramatically influence movement in cases where wind speed exceeds (or is comparable to) the animal's airspeed.

I investigated the effect of surface-level trade winds on genetic structure and gene flow in two species of bats in the Bahamas and Greater Antilles: *Erophylla sezekorni* (the buffy flower bat) and *Macrotus waterhousii* (Waterhouse's leaf-nosed bat) (Chiroptera: Phyllostomidae). *Erophylla* is one of the most common genera of plant-visiting phyllostomid bats in the Greater Antilles. The genus contains two currently recognized species: *E. sezekorni* (the buffy flower bat), distributed in the western Greater Antilles (Cuba, Jamaica, the Caymans, and Bahamas), and *E. bombifrons* (the brown flower bat) that occurs in the eastern Greater Antilles (Hispaniola and Puerto Rico) (Simmons 2005;

Koopman 1993). Recent molecular data, however, suggest that *Erophylla* contains a single species (*E. sezekorni*) with two major clades (the *sezekorni* and *bombifrons* clades) (Fleming *et al. in press* and *unpublished data*). I will treat all populations of *Erophylla* as belonging to a single species. These bats are members of the endemic subfamily Phyllonycterinae, which is thought to have lived in the Greater Antilles for as long as 11 million years (Davalos 2004).

Observations in the Greater Antilles indicate that *Erophylla* bats typically live in caves sometimes containing tens of thousands of individuals of several species living under very warm ($\leq 40^{o}$ C) and humid conditions (Silva Taboada 1979, Rodriguez-Duran 1995). Colony sizes of *Erophylla* in these caves range from a few hundred to a few thousand individuals. In the Caymans and Bahamas, in contrast, *E. sezekorni* lives in relatively cool caves and usually in colonies of a few bats to a few hundred individuals (Hall *et al.* 1998, K. Murray and T. Fleming, *pers comm*). Mating occurs in December-January throughout the Greater Antilles, and females give birth to a single pup in mid-June through at least late July (Silva Taboada 1979). Sex ratios in three caves on Exuma in the mating season and the maternity season are 1:1 (K. Murray, *pers. comm.*). Males and females apparently do not live in separate caves during the maternity period, in contrast to many other species of bats. The head/body and forearm lengths of adults are 65-75 mm and 41-55 mm, respectively (Baker *et al.* 1978; Nowak 1994).

In a recent study, Fleming *et al.* (*in press*) used D-loop mtDNA sequence data to demonstrate strong subdivision of *E. sezekorni* between the eastern islands of its range (Hispaniola and Puerto Rico) and the rest of the Greater Antilles. Haplotypes were shared extensively within the two clades but only two out of 34 total haplotypes (6%)

were shared between clades. Based on these data, the authors rejected the hypothesis of island monophyly, suggesting contemporary gene flow among islands. The long residence time of this species in the region makes this explanation more parsimonious than incomplete lineage sorting (Fleming *et al. in press*).

Bats of the genus *Macrotus* have a more widespread distribution than *Erophylla*, occurring throughout the Bahamas and Greater Antilles as well as on the Mexican mainland from northwestern Mexico south to Guatemala (Nowak 1994; Genoways *et al.* 2005). *Macrotus* is considered the basal genus of Phyllostomidae according to the molecular phylogeny of Baker *et al.* (2003) and has been aged at 28-34 million years (Jones *et al.* 2005; Teeling *et al.* 2005). Of the two currently recognized species, only *M. waterhousii* occurs in tropical dry forest habitats of Mexico as well as the Greater Antilles and Bahamas. Colonies of dozens or hundreds roost primarily in caves, although buildings and mines are occasionally used (Anderson 1969). Adults weigh 12-20 grams and the head/body and forearm lengths are 50-69 mm and 45-58 mm, respectively. Fleming *et al.*'s (*in press*) recent analysis showed that island populations of this species appear to be monophyletic in the Greater Antilles, indicating limited gene flow among islands.

The purpose of this study was to address the following questions: (1) What are the patterns of genetic structure throughout the Bahamas and Greater Antilles for these two species? (2) How much gene flow occurs among genetic populations in each of these species and is this gene flow symmetric or asymmetric? (3) Is there a detectable signal of wind-mediated gene flow for these species, among these islands? More precisely, does

the anisotropic effect of surface-level trade winds help explain instances of asymmetric gene flow between genetic populations?

I predicted wind to mediate gene flow of these species because of the energetic effects it has on flight dynamics. Specifically, I predicted that anisotropic measures of distance that incorporate the influence of wind would be more strongly correlated with genetic differentiation than Euclidean distance alone. This is one of only a few studies to employ anisotropic cost modeling in the context of evaluating genetic structure and gene flow. It is the first study to address these questions with a volant organism and to use this particular suite of approaches in unison.

Chapter 2: Materials and Methods

Sample Collection and Lab Procedures

Tissue samples were obtained throughout the Greater Antilles from 15 islands for *E. sezekorni* and 8 islands for *M. waterhousii* (Figure 1). In addition, tissue samples from three mainland sites in Mexico were obtained for *M. waterhousii*. Bats were captured with extendable hand nets inside caves or with mist nets set at cave entrances. Age, sex, reproductive status, body mass (g), and forearm length (mm) was recorded for most captured individuals. A small piece of tissue (2-20 mg) was clipped from the trailing edge of the wing and stored in 95% ethanol until analyzed in the lab.

Genomic DNA was extracted from 5 mg pieces of wing tissue using a standard ethanol precipitation procedure or DNeasy® DNA isolation kits (Qiagen) and stored in 50 μl of Tris-HCl, pH 8.5. We used polymerase chain reaction (PCR) and fluorescent dye-labeled primers (Tables 1 and 2) to amplify microsatellite fragments. Primers were developed commercially by Genetic Identification Services (www.genetic-id-services.com). Total PCR volume was 10 μl, with 1.0 μl Promega 10X buffer (2.5 mM $MgCl_2$ added), 0.8 units *Taq* DNA polymerase (Promega), 0.1 mM dNTPs. We combined primers from two or more loci (multiplexing) to amplify multiple loci simultaneously. Primer concentration (2.8 pmol to 5.6 pmol) and annealing temperature (50°C to 55°C) varied depending on the primer set used. PCR conditions were: initial denaturation at 94 °C for 2 min, followed by 30 cycles of 94 °C for 20 s, 50 °C (or 55 °C) for 20 s, and 72°C for 30 s, with a final elongation step at 72 °C for 5 min. PCR products were diluted with 30 μl (*E. sezekorni*) or 60 μl (*M. waterhousii*) of H_2O. We often mixed PCR products from different PCR reactions (coloading) to maximize the number of loci

we could analyze simultaneously. We added 0.5 μl of diluted PCR products to 10 μl size standard-formamide mix (0.01 μl GeneScan™ -500 LIZ™ size standard per 1ml of Hi-Di™ Formamide; Applied Biosystems, Inc.). All samples were analyzed and on an ABI 3730 automated sequencer and scored with GENEMAPPER software (Applied Biosystems, Inc.).

Table 1. Characterization of dye-labeled microsatellite primer pairs from *E. sezekorni*.

Locus	Sequence (5'-3')	T_a (°C)	Repeat motif
ES6	F: **6FAM**-TTCAGACCCACCCCATAAC R: AAGGGAACCATCATTTAGGC	50	$(AAT)_9$
ES8	F: **VIC**-AAGGGAAGGGGACATTTCT R: GGGAAGGTGAGGACAACTG	55	$(ATGT)_8$
ES17	F: **6FAM**-AAGTCCCACAGATACTCATCC R: AGAACCAGTGTCAAGAGAAAAC	55	$(TAGA)_{10}$
ES19	F: **VIC**-ATCTGGATACCTTCTGGAGAGT R: CCAAACAGCAGGACTTCC	55	$(TAGA)_7$
ES22	F: GGGTCATCTGTCCCTTATTC R: **NED**-ACTTCCTGCGTGTTTCAGT	55	$(TATC)_{10}$
ES24	F: GGACATCAGCATCACTAATTG R: **PET**-TCCTTACCACGTCTACTTGAGT	55	$(TAGA)_8$
ES27	F: **PET**-TACCTCGGACAATCTGTTGA R: AGCACCACCACTTTTGAAA	50	$(TAGA)_8$
ES35	F: **VIC**-ATCCCCTCCTTCATTCACTCT R: AGGCTGCTCCATAAATCAAGA	55	$(CA)_{15}$
ES38	F: **6-FAM**-CCATTCATTTTACCGTTTCAG R: GCAACTTGTTCTCATCACTTTG	55	$(CA)_{17}$
ES40	F: **NED**-AGGCAGTAGATTTTAGACAGTG R: ATGGTGACAATGGTGATG	55	$(GT)_{16}$
ES43	F: **PET**-ACCCGAACAGTTACTGAAAAAG R: GAAGACTTCCCCAGAACACTTA	55	$(CA)_{16}$
ES46	F: GGTTCCAGGCAGTTACTACTTA R: **VIC**-AGCCAGATTGTATCAGTTCTTC	55	$(ACC)_4(AAT)_{11}$

Table 2. Characterization of dye-labeled microsatellite primer pairs from *M. waterhousii*.

Locus	Sequence (5'-3')	T_a (°C)	Repeat motif
MW5	F: GAGACGAGCCATAAACAAGTT R: **6FAM**-ACCCCTCCTGCTTAGACC	50	$(AAT)_{12}$
MW11	F: **NED**-TATGGTCCCAAGGTCTCTTTAC R: CTGCCTCTTTCTTCATTCTCTC	50	$(TATG)_{11}$
MW15	F: GCAATGGTCAACACCTAAGG R: **6FAM**-CCCACAGAAACCGTGAGA	50	$(TATG)_{10}$
MW17	F: **VIC**-TTACCCCTAGAGCTTCACAA R: TCTCAAATTCTCACCGTCTAA	50	$(TAGA)_{12}$
MW18	F: **6FAM**-TGTCCTGGCAATACTTACATAA R: AAAGAAAGAAGGGCTCAGAG	50	$(TAGA)_{13}$
MW21	F: **PET**-ATGAATGTTGGTTCTGGTAGTC R: TGGGCTTATGCTCCTAAAC	50	$(TAGA)_{11}$
MW22	F: **PET**-CTTGCCCACCTCCATAGT R: CCAGAGAAACAGAATGAATAGC	50	$(TAGA)_{12}$
MW23	F: **NED**-CGAGCTAAAAGTAACCTGGTCT R: CCTACCTTCAAGGAGTTTATGG	50	$(TATC)_{9}$
MW24	F: **6FAM**-AGCCTAGCTGGGAGTATTTTT R: TTGTTTCACACACAGATGTTTC	50	$(TAGA)_{15}$
MW28	F: **VIC**-TTCCAGGAGAGGATTGATAAA R: CTGAAGATAGAGGGGTGACAG	50	$(TAGA)_{10}$

Genetic Data Analysis

The full dataset included 301 *E. sezekorni* individuals from 15 islands genotyped at 12 microsatellite loci and 204 *M. waterhousii* individuals from 11 locations (8 islands and 3 sites in mainland Mexico) genotyped at 10 microsatellite loci. I pooled *E. sezekorni* samples from Grand Cayman and Cayman Brac due to low sample sizes (but see Results § Genetic Structure). Standard population genetic statistics such as number of alleles per locus, number of private alleles, allelic richness, observed and expected heterozygosity, F_{IS} and pairwise F_{ST} values were computed using the programs FSTAT (Goudet 2001) and Arlequin 3.1 (Excoffier *et al.* 2005).

I tested *E. sezekorni* for genetic signals of sex-biased dispersal (there was not adequate sex information to test for sex-bias in *M. waterhousii*) by implementing seven independent tests of differential genetic divergence among males and females: F_{IS}, F_{ST}, Relatedness (r), observed (H_o) and expected (H_e) heterozygosity, mean assignment index (mA_I) and variance of assignment index (σA_I) (Goudet 2001; Goudet *et al.* 2002). In this study, relatedness was calculated as $2F_{ST}/(1+F_{IT})$ and has the same properties of the test based on F_{ST} (Goudet 2001). Mean assignment index is the average probability within a group (sex) that a genotype sampled in that group occurs more likely than average in that group. Immigrants would tend to have lower A_I values than residents, so under sex-biased dispersal, the dispersing sex should have a lower average A_I value than the more philopatric sex. The variance of A_I should be greater for the dispersing sex because members of this sex will include both residents and immigrants, as opposed to the more philopatric sex, which will primarily include residents. Significantly different values between the sexes for any of these parameters may indicate sex-biased gene flow.

Statistical significance was accessed using the randomization procedure described by Goudet (2001). All tests of pairwise differentiation, Hardy-Weinberg proportions and sex-biased dispersal were performed in FSTAT with 10^4 randomizations.

Genetic Structure

I used the program STRUCTURE (Prichard *et al.* 2000) to identify genetically distinct subpopulations within the study area. This program uses a Bayesian clustering analysis with multilocus genotype data to infer the number of independent genetic populations (K). The program assumes that loci are in Hardy-Weinberg and linkage equilibria within genetic populations. For the *E. sezekorni* dataset, I performed five independent trials of K=1-7 at $50x10^5$ Markov Chain Monte Carlo (MCMC) generations following a $50x10^4$ burn-in period using the admixture model and assuming correlated allele frequencies for all runs. I used the same procedure with K=1-14 for the *M. waterhousii* analysis. Prior population information was not included in the analysis, and all other parameters were set to the default values. Appropriate run length was determined based on suggestions in the STRUCTURE documentation (Prichard *et al.* 2000). I selected the value of K to use in subsequent gene flow analyses based on the maximum estimated log-likelihood of $P(X \mid K)$ averaged across independent trials. After determining the total number of separate genetic populations (K) for each species in the study area, I assigned islands to each of the K groups based on the maximum estimated membership coefficient (q-value) averaged across individuals within islands. I used additional runs with subsets of the data for islands with ambiguous membership (see Results § *Genetic Structure*).

Geographic Information System

I obtained an unprojected base map of the study area from the Digital Chart of the World Server (http://www.maproom.psu.edu/dcw/) (Figure 1). While viewing the map with the equidistant conic projection, I used the Distance/Azimuth between Matched Features v.2 extension (Jenness 2004) in ArcGIS version 9.1 (ESRI 2002) to find the line connecting the nearest edges of all island pairs. I recorded distance (D_{GEO}) and azimuth (degrees clockwise from north) of these lines. The shortest distance between island groups was determined as the minimum distance between all possible island pairs within groups. I recorded island area (km^2) and group area as the sum of island areas included in the group. I imported the base map into IDRISI Andes (Clark labs 2006) and used the RASTERVECTOR module to convert it into a 225 by 153 grid cell image for all raster-based analyses.

Wind Data

I used surface wind data from the National Climatic Data Center (ftp://ftp.cdc.noaa.gov/pub/Datasets), which includes monthly mean magnitude and direction from 1948 to 2005 at 2.5° lat/long (≈278 km^2) resolution (Figure 2). Data were available for all months except November and December. To explore seasonal variation in the wind data, I plotted mean magnitude and direction versus month for three locations (22.5°N; 82.5°W, 17.5°N; 77.5°W and 17.5°N; 70°W) within the study area. Climatological monthly mean winds were derived from the annual monthly means provided in the NCDC dataset by calculating the mean wind magnitude and direction for each month. A similar temporal pattern was evident at these locations, and neither speed

nor direction changed dramatically during the year (Figure 3a,b). All subsequent analyses were performed with wind data averaged across all available months (ANNUAL) as well as with the data from June (JUNE), the month of peak wind speeds and . I generated raster images with cells containing wind speed and direction for the annual and June periods at the same resolution as the base map.

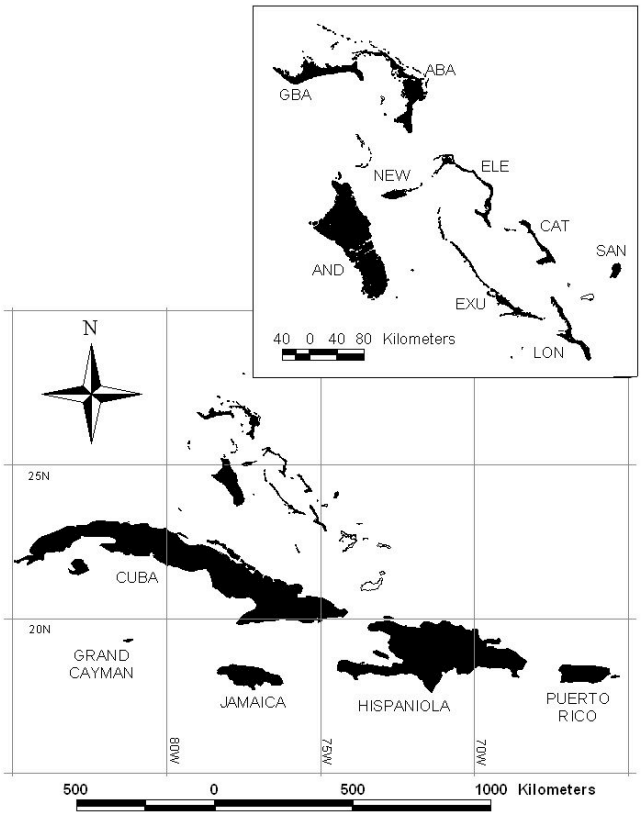

Figure 1. Map of the study area. Unsampled islands are white. Inset shows the Bahamas: ABA=Abaco, AND=Andros, CAT=Cat Island, ELE=Eleuthera, EXU=Exuma, GBA=Grand Bahama, LON=Long Island, NEW=New Providence and SAN=San Salvador.

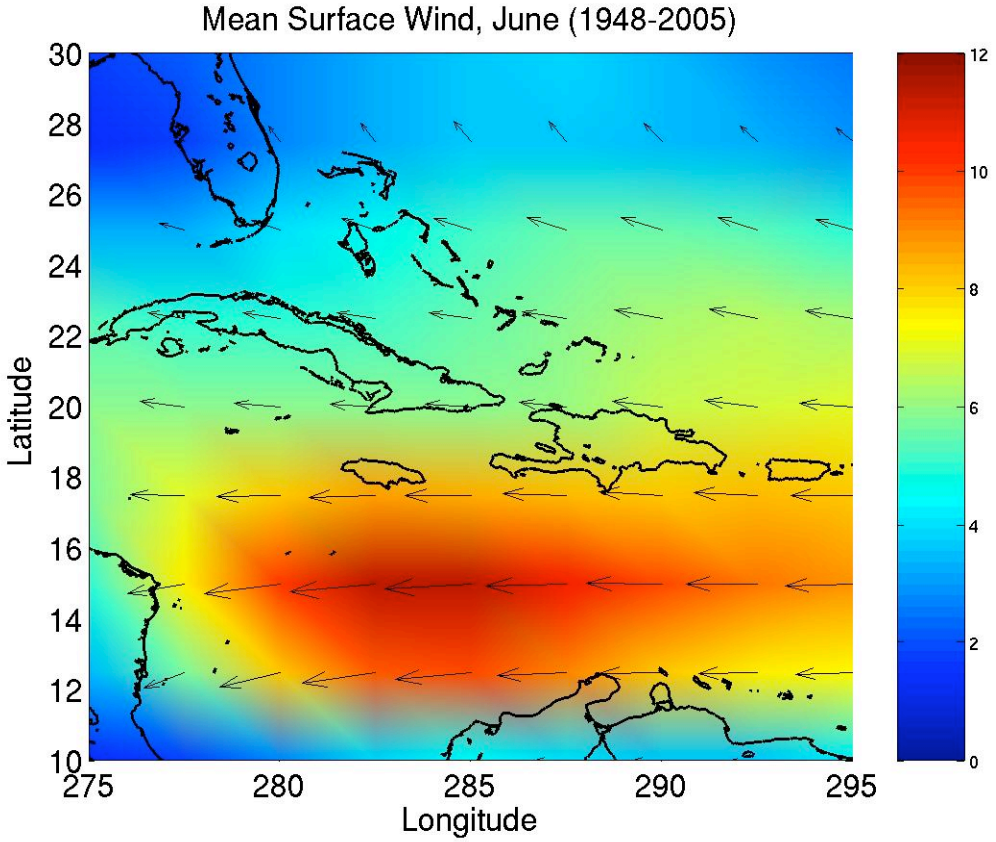

Figure 2. Graphical representation of mean surface winds in the study area during the month of June from 1948 to 2006. Scale shows wind magnitude in m/s. Data are from the National Climatic Data Center (ftp://ftp.cdc.noaa.gov/pub/Datasets).

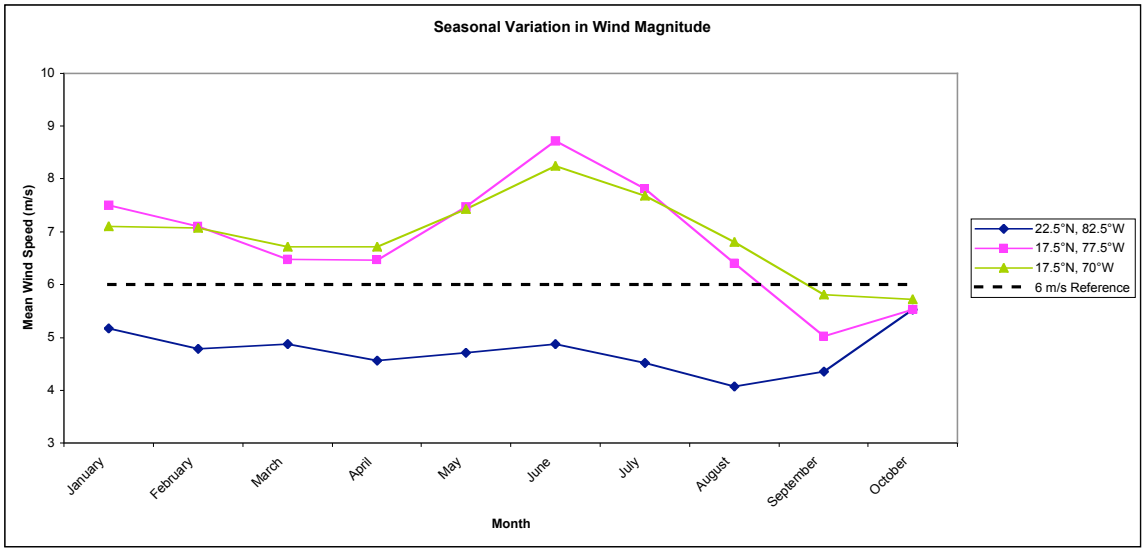

Figure 3a. Time series plot of mean wind magnitude (m/s) at three locations within the study area. Data are from the National Climatic Data Center (ftp://ftp.cdc.noaa.gov/pub/Datasets). Dashed line is included as a 6 m/s reference.

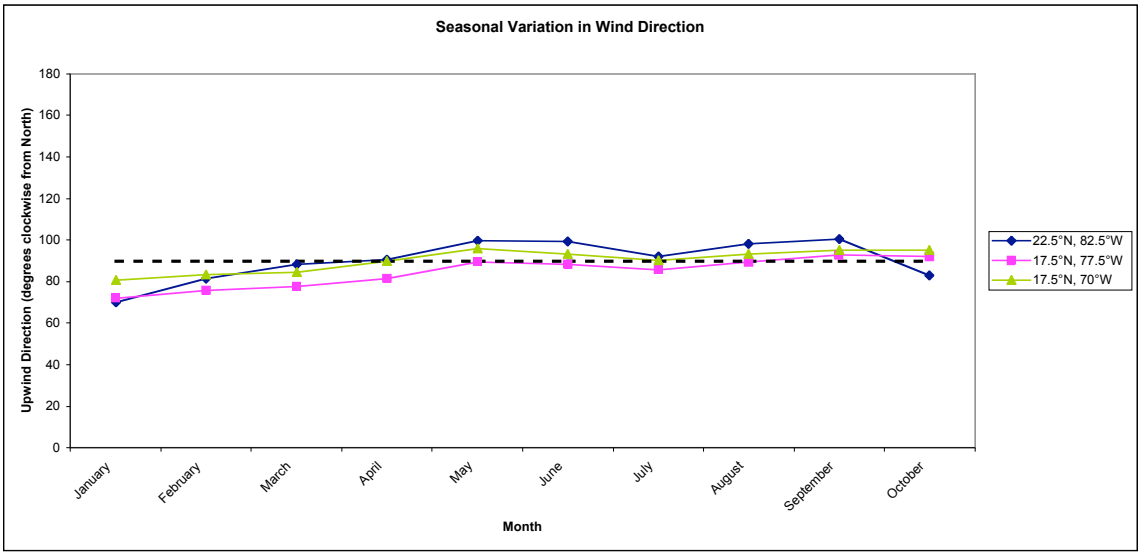

Figure 3b. Time series plot of mean wind direction (degrees clockwise from north) at three locations in the study area. Direction value indicated *upwind* direction. Data are from the National Climatic Data Center (ftp://ftp.cdc.noaa.gov/pub/Datasets). Dashed line is included for a 90° (east) reference.

Anisotropic Cost Analysis

Anisotropic cost analysis is a method for estimating the travel cost from a source cell to every other cell on a grid when there are directional forces at play. The analysis generates a relative value of effective distance between features of interest which can be asymmetrical between two given features. I considered fields of wind vectors as a friction surface for this analysis. Movement from one grid cell to another along the exact wind azimuth received a minimum cost that was the inverse of the magnitude of wind speed. Deviations from the exact wind azimuth were treated by a function, called the anisotropic function, which incrementally penalized angular deviations from the wind azimuth up to 180º with increased cost to movement. For both periods (ANNUAL and JUNE), I used the default anisotropic function provided in IDRISI (Clark labs 2006) for these calculations:

(1) Effective friction = stated friction^f

where f = $\cos \alpha$
and α = the difference angle

The difference angle (α) is the angle between the direction being considered (i.e. the azimuth of the shortest line between islands) and the direction *from which* frictions are acting (i.e. directly upwind direction) (Clark labs 2006). I used effective friction to calculate effective distance, D_{Wij}:

(2) D_{Wij} = (effective friction) x (D_{GEO})

Initially, I used the VARCOST anisotropic cost module for the anisotropic cost analysis. This module requires three input images with matching resolution: one binary

map containing the feature of interest (source island) and two images with grid cells corresponding to the magnitude and direction of the force, respectively. The result is a cost surface image between a user-defined source feature and every other cell of the grid. Unfortunately, trial runs with simulation data showed that this module did not function properly for my question. For example, it did not result in the predictable 'plume' of low effective distance downwind from the source feature. I found these erroneous results when any angle besides cardinal or intercardinal directions was used in the direction image.

I developed an alternative approach to get around this problem. For each island, I used the DISTANCE module to generate an image with grid cells containing Euclidean distance away from the source island. I used the PATHWAY module with each distance image as a 'cost surface'. This resulted in separate binary images of the shortest route between all island pairs. I used the EXTRACT module to find the average wind magnitude and direction values for the cells included in these routes. In contrast to the VARCOST module, which provides the effective distance of the route that minimizes wind resistance between islands, this procedure resulted in the average magnitude and direction of wind that would be encountered when traveling along the shortest route between islands. I believe that this method provides more biologically meaningful results than the VARCOST module. I performed this analysis between all island pairs using ANNUAL and JUNE wind speed and direction data. The results of these analyses were distance matrices for each period that could be asymmetrical between islands (i.e. $D_{Wij} \neq D_{Wji}$). I evaluated the degree of asymmetry of effective distance for both periods with an index of D_W asymmetry for all island pairs (i,j):

$$(3) \qquad R_{Dw\,(ij;ji)} = \frac{|\, D_{Wij} - D_{Wji} \,|}{|\, D_{Wij} + D_{Wji} \,|}$$

R_{Dw} ranges from 0 to 1; a value of 0 indicates complete symmetry and a value of 1 indicates complete asymmetry. This index incorporates information about the spatial configuration of island pairs relative to mean wind direction.

Gene Flow

I estimated magnitude and polarity of gene flow between genetic populations using the maximum likelihood approach implemented in MIGRATE v.2.13 (Beerli and Felsenstein 2001). MIGRATE uses a coalescence approach to estimate population genetic parameters assuming mutation-migration-drift equilibrium and constant values of migration, theta (effective population size) and per-locus mutation rate. Under these frequently unrealistic assumptions, it is best to view parameters estimated by this program as long-term estimates (Hanfling and Weetman 2006). This approach is generally considered to provide more accurate estimates of gene flow than F_{ST} methods (Whitlock and McCauley 1999; Beerli and Felsenstein 1999; Beerli 2004). MIGRATE uses a default *n* x *n* island migration model that was inappropriate for this study. Given the large spatial scale of this study, gene flow between distant islands (for example, between Jamaica and Abaco in Figure 1) is far less parsimonious than gene flow among islands in a stepping-stone fashion. I created a stepping-stone model of gene flow among islands by visually inspecting the shortest line between island or group pairs to determine pairs where this line was intersected by another island. Pairs with another island

intersecting this line were excluded from the migration matrix by constraining the migration parameter to zero. I determined the run length necessary to achieve consistent results following the suggestions in the MIGRATE manual and through communication with the program's creator (Beerli and Felsenstein 2001; P. Beerli *pers comm*). I initially ran the program with the Brownian motion approximation and all other settings as defaults. I then used the output parameter estimates as start values for a second run. The datasets for the two species required separate optimization of run times because of different sample sizes and migration matrices. Results presented here for *E. sezekorni* are from 20 short chain searches ($25x10^4$ trees sampled, $5x10^3$ trees recorded) followed by 3 long chain searches ($25x10^5$ trees sampled, $5x10^4$ trees recorded) after a 10^4 burn-in period and using the Brownian motion approximation. *M. waterhousii* results are from 15 short chain searches ($2x10^4$ trees sampled, 10^3 trees recorded) followed by 3 long chain searches ($5x10^5$ trees sampled, 10^3 trees recorded) after a 10^4 burn-in period and using the Brownian motion approximation. The results of the final long chain search were averaged over three independent runs. I identified instances of asymmetrical migration rates between the island pairs by examining the 95% confidence intervals of these migration parameters estimated using the 'quick' method. I calculated an index of gene flow asymmetry (R_{Nm}) for island or group pairs:

$$R_{Nm(ij;ji)} = \frac{| N_{mij} - N_{mji} |}{| N_{mij} + N_{mji} |} \quad (4)$$

R_{Nm} ranges from 0 to 1; a value of zero indicates complete symmetry and a value of one indicates complete asymmetry. All pairs with overlapping 95% confidence intervals of migration rate were assigned a value of zero.

Isolation by Distance

As predicted when populations are in drift-migration equilibrium, I tested for a positive linear relationship between pairwise genetic differentiation ($F_{ST}/(1-F_{ST})$) and the natural log of Euclidean distance (Rousset 1997) between islands and groups for *E. sezekorni* and between islands for *M. waterhousii* (IBD_{GEO}). Positive residual variation from these analyses indicates island or group pairs with greater genetic divergence than predicted by Euclidean distance alone, whereas negative residual variation reflects lower genetic divergence than predicted by distance. If wind mediates this pattern, island and group pairs with negative residuals should be configured relative to the mean wind such that wind increases gene flow between them, at least in one direction (i.e., they are configured parallel to mean wind direction). I tested for a significant difference in the absolute value of relative configuration (α from the anisotropic function) between island and group pairs with negative and positive IBD residuals using a T-test. I also performed a randomization test to determine if the slope of the regression line fitted to the subset of island pairs included in the migration matrix differed significantly from the slope fitted to all island pairs.

If mean surface winds mediate gene flow, genetic differentiation should be more strongly correlated with a measure of effective distance than with simple Euclidean distance. Because typical measures of genetic differentiation (F_{ST}) are symmetric (a

single value for two groups) and F_{ST} declines rapidly with a few migrants, F_{ST} should be governed by the minimum effective distance between islands. I examined the correlation between genetic differentiation and the natural log of minimum D_{WIND} for each island (and group) pair. As an alternative approach to examine the effect of wind on gene flow between genetic populations, I compared the degree of asymmetric gene flow (R_{Nm}) to the degree of distance asymmetry (R_{Dw}) for each group (*E. sezekorni*) and island (*M. waterhousii*) pair . Statistical significance of all IBD relationships was assessed using Mantel tests (Mantel 1967) performed for 10^4 randomizations in FSTAT; 95% confidence intervals of IBD slopes were computed with the online program IBD (Jensen *et al.* 2005).

Chapter 3: Results

Genetic Structure

E. sezekorni

In several preliminary runs of STRUCTURE, samples from Grand Cayman and Cayman Brac appeared to behave as independent populations. Sample size from these islands was inadequate to make genetic structure inferences, however (n=8 and 3, respectively), so I excluded these samples from the remaining analyses. Estimated log likelihood values for the remaining 13 island dataset peaked at K=5 (mean -11484 +/- SD 12.71). Clustering islands based on the maximum proportion of membership to each of the 5 hypothesized populations revealed 4 distinct groups: (1) Abaco and Grand Bahama, (2) Andros, Cat Island, Cuba, Eleuthera, Exuma, Long Island, New Providence and San Salvador, (3) Hispaniola and Puerto Rico, and (4) Jamaica. No island, however, was assigned with a maximum proportion of membership to one of the five hypothesized populations as determined appropriate by the log likelihood values. In order to refine island groupings, I reran STRUCTURE using subsamples of the original dataset. I first removed samples from Hispaniola and Puerto Rico from the data set and ran the program for the remaining 11 islands for K=1-4. The maximum log likelihood value occurred at K=3 (-9183 +/- SD 10.3). Jamaican samples were clearly identified as a subpopulation in this run ($q > 0.9$). Because the Bahamian islands and Cuba had already been grouped into two populations, these results suggested presence of additional genetic structure within the two eastern islands (Hispaniola and Puerto Rico). Running the program with only these eastern islands for K=1-3 revealed a maximum log likelihood value at K=2 (-1734 +/- SD 2.4), suggesting genetic structure between Hispaniola (HIS) and Puerto Rico

(PUE). Between these two islands, HIS showed substantially greater admixture (i.e. individuals captured had a greater proportion membership for the PUE subpopulation than vice versa), suggesting asymmetric gene flow from PUE to HIS. The final island groups were (1) Little Bahama Bank (LBB): Grand Bahama and Abaco, (2) Great Bahama Bank (GBB): Andros, Cat Island, Cuba, Eleuthera, Exuma, Long Island, New Providence and San Salvador, (3) Hispaniola (HIS), (4) Puerto Rico (PUE) and (5) Jamaica (JAM) (Figure 4). Because it contains Cuba and San Salvador, GBB in this paper is larger than the geologically defined Great Bahama Bank.

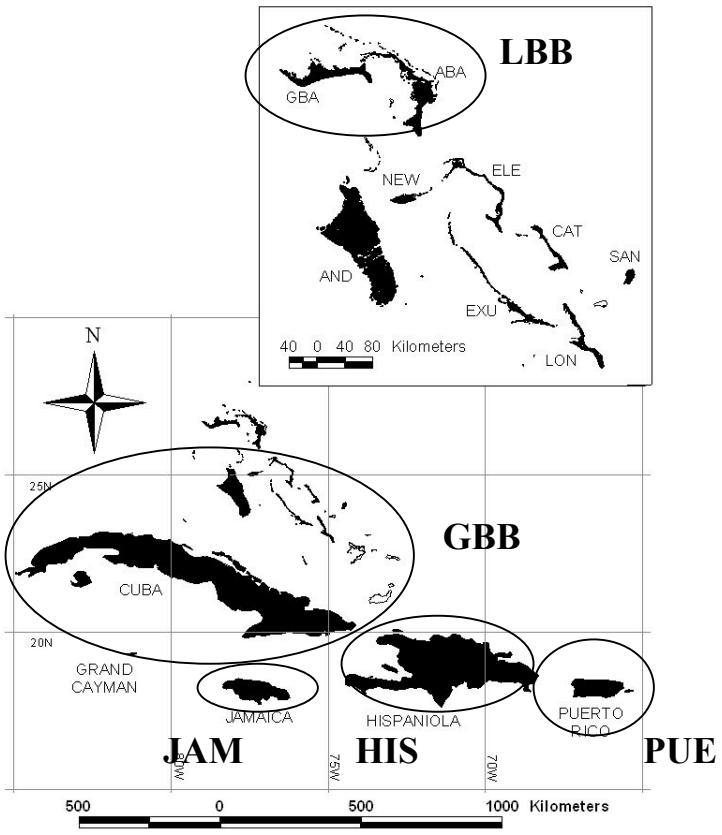

Figure 4. The five genetic populations of *E. sezekorni* as determined by STRUCTURE analysis: LBB=Little Bahama Bank, GBB=Great Bahama Bank, JAM=Jamaica, HIS=Hispaniola and PUE=Puerto Rico.

M. waterhousii

Estimated log likelihood values for the 11 sample sites peaked at K= 11 (-7095.6 +/- SD 103.2). Maximum average q-values for sites ranged from 0.58 to 0.95 (mean 0.83 +/- SD 0.11), and all 8 islands had a maximum average q-value of >0.7. Based on these results, all sample islands were assigned to separate hypothetical populations. Overall, this analysis showed that island populations of *M. waterhousii* are genetically distinct from each other and represent independent genetic populations (Figure 5). Because no two islands clustered together, all further analyses for this species were carried out among islands only.

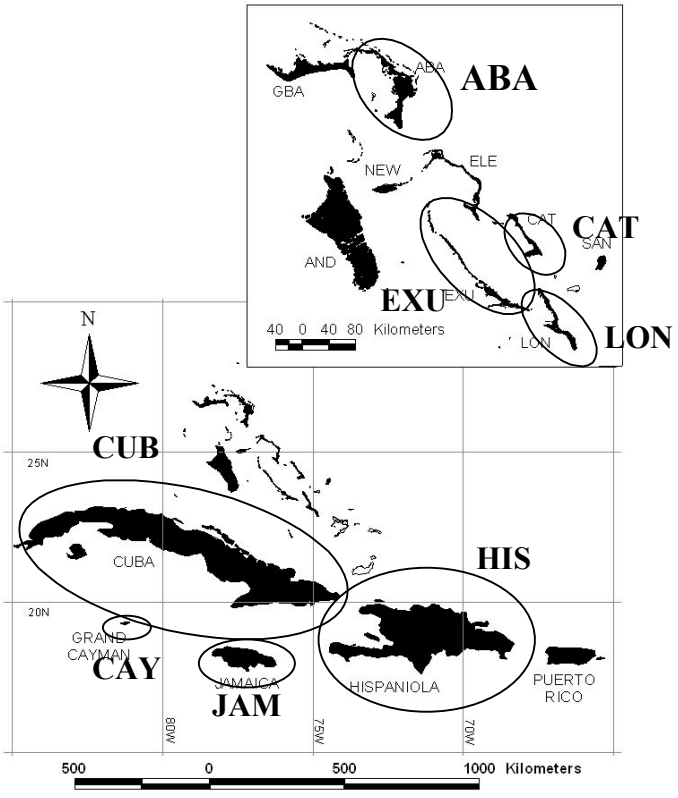

Figure 5. The eight genetic populations of *M. waterhousii* as determined by STRUCTURE analysis. Each island sampled for this species represents an independent genetic population.

Genetic Diversity and Differentiation

E. sezekorni

Microsatellite marker characteristics for the 14 islands sampled for the *E. sezekorni* dataset are shown in Table 3. In total, 142 alleles were detected at 12 loci from all genotyped individuals (n=301). The total number of alleles per locus ranged from 6-24 (mean 12.9 +/- SD 5.17). There was no evidence of linkage disequilibrium in the 66 locus-pair tests.

Table 3. Sample size (N), number of alleles (N_A), number of private alleles (N_P), mean allelic richness (A_R), observed (H_o) and expected (H_e) heterozygosity and estimates of inbreeding coefficient (F_{IS}) over all loci for *E. sezekorni* among islands (a), groups (b) and *M. waterhousii* among islands (c). Significant ($p<0.05$) deviations from H-W equilibrium are indicated in **bold**. See Figures 1, 4 and 5 for location abbreviations. Mexican mainland locations for *M. waterhousii* are designated by (*ML*) and are COL=Colima, PBL=Puebla, and SON=Sonora.

a. *E. sezekorni* – Islands

	ABA	AND	CAT	CAY	CUB	ELE	EXU	GBA	HIS	JAM	LON	NEW	PUE	SAN
N	20	22	27	8	18	31	25	20	28	15	25	25	24	13
N_A	71	90	85	40	90	87	86	71	78	70	85	84	59	71
N_P	0	1	1	0	5	0	2	0	5	2	1	1	0	2
A_R	4.8	5.6	5.3	3.3	5.7	5.5	5.6	4.9	5.0	4.7	5.3	5.5	4.0	5.2
H_o	0.71	0.74	0.73	0.56	0.73	0.75	0.75	0.67	0.66	0.62	0.72	0.74	**0.59**	0.70
H_e	0.71	0.75	0.74	0.58	0.75	0.74	0.75	0.70	0.69	0.65	0.72	0.76	**0.62**	0.71
F_{IS}	0.00	0.01	0.02	-0.07	0.03	-0.01	0.02	0.07	0.06	0.05	0.00	0.03	0.06	0.01

b. *E. sezekorni* – Groups

	LBB	GBB	HIS	JAM	PUE
N	40	186	28	15	24
N_A	80	129	78	70	59
N_P	0	27	5	2	0
A_R	5.6	6.8	5.7	5.7	4.5
H_o	0.69	0.73	0.66	0.62	0.59
H_e	0.70	0.76	0.69	0.65	0.62
F_{IS}	0.04	0.03	0.06	0.05	0.06

c. *M. waterhousii* – Islands and mainland (*ML*)

	ABA	CAT	CAY	COL (*ML*)	CUB	EXU	HIS	JAM	LON	PBL (*ML*)	SON (*ML*)
N	20	26	11	18	11	39	32	24	27	28	9
N_A	36	54	38	51	52	61	73	70	55	39	32
N_P	0	0	2	2	1	0	8	12	0	1	2
A_R	2.6	3.3	2.8	2.9	3.5	3.3	3.6	3.7	3.3	2.5	2.5
H_o	0.64	0.69	0.69	0.67	0.73	0.69	0.73	0.71	0.73	0.54	0.50
H_e	0.60	0.72	0.72	0.66	0.77	0.72	0.77	0.78	0.73	0.56	0.56
F_{IS}	-0.07	0.04	0.06	-0.03	0.06	0.04	0.05	0.09	0.01	0.04	0.10

Island level parameters

In total, 20 private alleles were detected (14% of total alleles). The number of private alleles per locus ranged from 0-7 (mean 1.67 +/- SD 1.87). Island samples had 0-5 private alleles (mean 1.43 +/- SD 1.70) with the maximum appearing on both Cuba and Hispaniola, the two largest islands sampled. Average observed heterozygosity over all loci was 0.69 and Hardy-Weinberg proportions occurred on all islands except Puerto Rico ($p=0.0001$), which had a heterozygote deficiency. The estimated total F_{IS} over all loci was 0.024 (95% CI -0.009–0.058). All pairwise tests of differentiation were significant after strict Bonferroni correction except between Abaco and Grand Bahama ($p=0.06$). Except for the F_{ST} test ($p<0.01$), tests for sex-biased gene flow were not significant, indicating that males and females probably contribute equally to gene flow in this species (Table 4a).

Group level parameters

There were 32 private alleles (23% of total alleles) detected among the five groups. The number of private alleles per group ranged from 0-26 (mean 6.4 +/- SD 11.1), with most (81%) appearing in the GBB group. Average observed heterozygosity over all loci was 0.66, and the estimated total F_{IS} over all loci was 0.039 (95% CI -0.007–0.072). Hardy-Weinberg proportions occurred in all groups ($p>0.05$), and all pairwise tests of differentiation were significant after strict Bonferroni correction. None of the tests for sex-biased gene flow showed statistical significance at this level of analysis ($p>0.05$) (Table 4b).

Table 4. Results for tests of sex-biased dispersal in *E. sezekorni* among islands (a) and groups (b). Relatedness is calculated as $2F_{ST}/(1+F_{IT})$ and has the same properties as the test based on F_{ST} (Goudet 2001). Mean assignment index (mA_I) is the average probability within a group (sex) that a genotype sampled in that group occurs more likely than average in that group. Immigrants tend to have lower A_I values than residents, so under sex-biased dispersal, the dispersing sex should have a lower average A_I value than the more philopatric sex. The variance of A_I should be greater for the dispersing sex because members of this sex will include both residents and immigrants, as opposed to the more philopatric sex, which will primarily include residents. Statistical significance of differences between the sexes for these indices was accessed using the randomization procedure described by Goudet (2001) in FSTAT with 10^4 randomizations.

a.

	N	**F_{IS}**	**F_{ST}**	***r***	**H_O**	**H_E**	**mA_I**	**σA_I**
Females	112	0.01	0.05	0.10	0.73	0.73	-0.12	6.77
Males	90	0.03	0.09	0.16	0.70	0.72	0.14	11.64
Total	202	0.02	0.07	0.13	0.72	0.73	--	--
p-*value*		ns	0.01	ns	ns	ns	ns	ns

b.

	N	**F_{IS}**	**F_{ST}**	***r***	**H_O**	**H_E**	**mA_I**	**σA_I**
Females	96	0.02	0.07	0.13	0.73	0.74	-0.49	11.15
Males	86	0.03	0.13	0.22	0.70	0.72	0.55	12.39
Total	182	0.02	0.10	0.18	0.71	0.73	--	--
p-*value*		ns	ns	ns	ns	ns	ns	ns

M. waterhousii

Microsatellite marker characteristics for the 11 sites sampled in the *M. waterhousii* dataset are shown in Table 3c. In total, 118 alleles were detected at 10 loci from the genotyped individuals (n=245). The total number of alleles per locus ranged from 9-19 (mean 11.8 +/- SD 3.04). There was no evidence of linkage disequilibrium in the 45 locus-pair tests. Allelic richness was substantially lower in *M. waterhousii* than in *E. sezekorni*.

Island level parameters

In total, 28 private alleles were detected among 10 sites sampled (24% of total alleles). The number of private alleles per locus ranged from 1-8 (mean 5.09 +/- SD 2.04). Sites had 0-12 private alleles (mean 2.55+/- SD 3.88) with the maximum appearing on Jamaica. Average observed heterozygosity over all loci was 0.67, and Hardy-Weinberg proportions occurred at all sites. The estimated total F_{IS} over all loci was 0.034 (95% CI -0.009–0.059). All pairwise tests of differentiation were significant ($p<0.05$) after Bonferroni correction.

Gene Flow

Neither effective population size (Θ) nor mean immigration rate was correlated with the natural log of island or group area with in either species. Migration rate and theta value estimates between genetic populations of *E. sezekorni* are shown in Table 5. Migration rate scaled for mutation rate ($M=m/\mu$) ranged from 0.08 – 15.31 (mean 5.04 +/- SD 5.23). Four of the five pairwise comparisons (80%) exhibited significantly asymmetric rates of gene flow based on non-overlapping 95% confidence intervals. Gene flow between HIS and GBB was symmetric and relatively low compared to the other pairs. The highest gene flow was between LBB and GBB, with greater gene flow from GBB to LBB than vice versa. Gene flow between PUE and HIS was also asymmetric, with significantly greater migration from PUE to HIS than vice versa. Gene flow between JAM and HIS was relatively low and asymmetric, with greater gene flow from JAM to HIS than vice versa.

Table 5. Theta ($N_e\mu$) (on diagonal in bold) and Migration rate scaled for mutation rate ($M=m/\mu$) (off diagonal) among genetic populations of *E. sezekorni* as determined by MIGRATE analysis. 95% confidence intervals are below maximum likelihood value in parentheses. Migration rates represent gene flow *FROM* the column locations *TO* the row locations. Group pairs excluded from the stepping stone migration model are indicated by (--) as migration was manually constrained to zero for these pairs. See Figure 4 for location abbreviations.

	LBB	GBB	HIS	JAM	PUE
LBB	**0.59**	15.31	--	--	--
	(0.56-0.63)	(14.02-16.69)			
GBB	10.36	**1.55**	1.10	10.90	--
	(9.60-11.15)	**(1.50-1.61)**	(0.87-1.37)	(10.10-11.73)	
HIS	--	1.67	**0.82**	0.52	7.68
		(1.26-2.16)	**(0.75-0.89)**	(0.31-0.81)	(6.75-8.67)
JAM	--	0.58	0.08	**12.72**	--
		(0.50-0.66)	(0.06-0.12)	**(11.90-13.64)**	
PUE	--	--	2.20	--	**0.81**
			(1.83-2.68)		**(0.75-0.88)**

Migration rate and theta value estimates among genetic populations of *M. waterhousii* are shown in Table 6. Migration rate scaled for mutation rate ($M=m/\mu$) ranged from 0.00 – 13.20 (mean 1.98 +/- SD 2.74). Twelve of the 15 island pairs (80%) included in the migration matrix displayed asymmetric gene flow based on non-overlapping 95% confidence intervals. Gene flow was relatively high and asymmetric between Cuba and all other islands included in the migration matrix. All of these instances showed immigration biased toward Cuba. The low sample size from Cuba (n=11) could limit the number of observed alleles and therefore theta, in turn resulting in a low number of estimated migrations (P. Beerli *pers comm*). I used two approaches to address this potential problem: (1) I randomly resampled 11 individuals from each other island and reran the program, and (2) I reran the program including only samples from Cuba, Hispaniola, Jamaica and Exuma. I used the same parameter settings as described above for both of these runs. The output of these runs yielded comparable results in that

migration was still biased *toward* Cuba (data not shown), suggesting adequate sample size from Cuba to achieve a reliable estimate for these parameters.

Table 6. Theta ($N_e\mu$) (on diagonal in bold) and migration rate scaled for mutation rate ($M=m/\mu$) (off diagonal) among genetic populations of *M. waterhousii* as determined by MIGRATE analysis. 95% confidence intervals are below maximum likelihood value in parentheses. Migration rates represent gene flow *FROM* the column locations *TO* the row locations. Group pairs excluded from the stepping stone migration model are indicated by (--) as migration was manually constrained to zero for these pairs. See Figure 5 for location abbreviations.

	ABA	CAT	CAY	CUB	EXU	HIS	JAM	LON
ABA	**0.74**	--	--	--	1.59	--	--	--
	(0.68-0.81)				(1.28-1.98)			
CAT	--	**0.95**	--	--	1.04	0.00	--	0.69
		(0.87-1.04)			(0.79-1.35)	(0.00-0.03)		(0.49-0.93)
CAY	--	--	**0.20**	0.00	--	1.80	2.19	--
			(0.17-0.22)	(0.00-0.14)		(1.18-2.59)	(1.48-3.08)	
CUB	--	--	5.70	**0.29**	13.21	2.03	4.10	5.56
			(3.98-7.86)	**(0.24-0.30)**	(10.46-16.41)	(1.08-3.41)	(2.66-6.00)	(3.86-7.69)
EXU	5.43	2.47	--	1.17	**0.90**	0.35	--	0.00
	(4.73-6.20)	(2.03-2.98)		(0.87-1.53)	**(0.84-0.97)**	(0.20-0.56)		(0.00-0.04)
HIS	--	0.00	0.95	0.00	2.98	**1.14**	0.84	1.98
		(0.00-0.05)	(0.67-1.30)	(0.00-0.05)	(2.45-3.59)	**(1.05-1.24)**	(0.58-1.18)	(1.56-2.47)
JAM	--	--	0.00	0.00	--	0.79	**2.74**	--
			(0.00-0.02)	(0.00-0.02)		(0.64-0.96)	**(2.50-3.01)**	
LON	--	0.00	--	1.01	3.25	0.13	--	**0.63**
		(0.00-0.06)		(0.70-1.40)	(2.66-3.93)	(0.04-0.29)		**(0.58-0.69)**

Isolation by distance

Pairwise F_{ST} and Euclidean distances between islands and groups of *E. sezekorni* and islands of *M. waterhousii* are shown in Tables 7 and 8, respectively. I detected significant IBD_{GEO} for *E. sezekorni* at both the island (R^2=0.537, p<0.0001) and the group level (R^2=0.607, p<0.001) (Figure 6a,b). Island pairs excluded from the migration matrix had significantly greater negative residual variation than island pairs included in the migration matrix (p<0.0001). The results of a randomization test, however, showed

no difference between the slope of the regression line for the subset of points included in the migration matrix and for the full data set (10^3 randomizations, $p>0.05$).

Table 7a. F_{ST} (above diagonal) and Euclidean distance in km (below diagonal) for *E. sezekorni* among islands (a) and groups (b). Significant ($p<0.05$) F_{ST} values are indicated by **bold** type.

	ABA	AND	CAT	CAY	CUB	ELE	EXU	GBA	HIS	JAM	LON	NEW	PUE	SAN
ABA	--	0.04	0.04	0.21	0.07	0.04	0.06	0.00	0.18	0.16	0.03	0.04	0.23	0.08
AND	102	--	0.01	0.19	0.04	0.02	0.03	0.02	0.15	0.14	0.03	0.01	0.21	0.05
CAT	195	191	--	0.15	0.04	0.00	0.03	0.03	0.17	0.14	0.01	0.01	0.22	0.04
CAY	822	592	783	--	0.16	0.15	0.16	0.20	0.27	0.27	0.17	0.17	0.34	0.16
CUB	384	139	312	260	--	0.03	0.05	0.06	0.17	0.09	0.03	0.03	0.21	0.04
ELE	50	111	39	775	309	--	0.03	0.03	0.16	0.12	0.01	0.00	0.22	0.03
EXU	119	89	68	695	226	47	--	0.06	0.16	0.16	0.02	0.04	0.21	0.04
GBA	3	136	292	827	400	148	214	--	0.19	0.15	0.03	0.02	0.24	0.07
HIS	771	608	511	704	85	600	446	868	--	0.21	0.18	0.16	0.09	0.20
JAM	813	571	649	309	145	692	565	886	189	--	0.14	0.13	0.25	0.16
LON	305	219	49	740	210	133	24	403	365	536	--	0.02	0.23	0.03
NEW	81	37	143	724	284	31	42	166	696	715	238	--	0.22	0.04
PUE	1315	1222	1049	1461	750	1151	1017	1411	114	946	932	1260	--	0.24
SAN	332	297	77	846	334	174	110	427	458	659	80	283	970	--

Table 7b.

	GBB	LBB	HIS	JAM	PUE
GBB	--	0.03	0.15	0.12	0.20
LBB	50	--	0.19	0.15	0.23
HIS	85	771	--	0.21	0.09
JAM	145	813	189	--	0.25
PUE	750	1315	114	946	--

Table 8. F_{ST} (above diagonal) and Euclidean distance in km (below diagonal) for *M. waterhousii* among islands. Significant ($p<0.05$) F_{ST} values are indicated by **bold** type.

	ABA	CAT	CAY	CUB	EXU	HIS	JAM	LON
ABA	--	0.16	0.22	0.17	0.14	0.17	0.16	0.16
CAT	195	--	0.19	0.12	0.11	0.13	0.10	0.11
CAY	822	783	--	0.15	0.19	0.15	0.15	0.15
CUB	384	312	260	--	0.12	0.09	0.05	0.08
EXU	119	68	695	226	--	0.12	0.10	0.07
HIS	771	511	704	85	446	--	0.11	0.11
JAM	813	649	309	145	565	189	--	0.08
LON	305	49	740	210	24	365	536	--

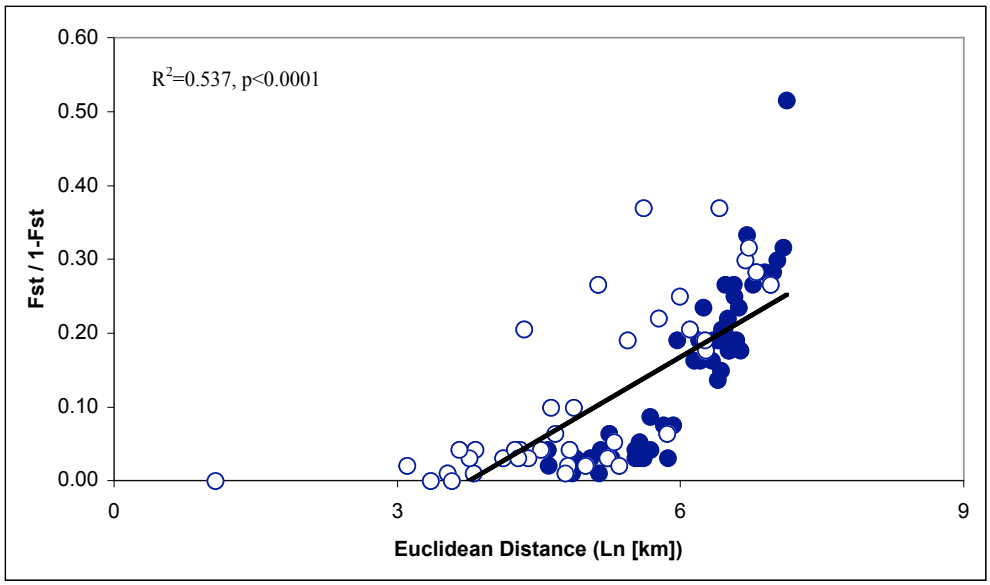

Figure 6a. Isolation by distance for *E. sezekorni* at the island level. Open circles represent island pairs included and filled circles represent island pairs excluded in the migration matrix. Regression line was fitted to all points.

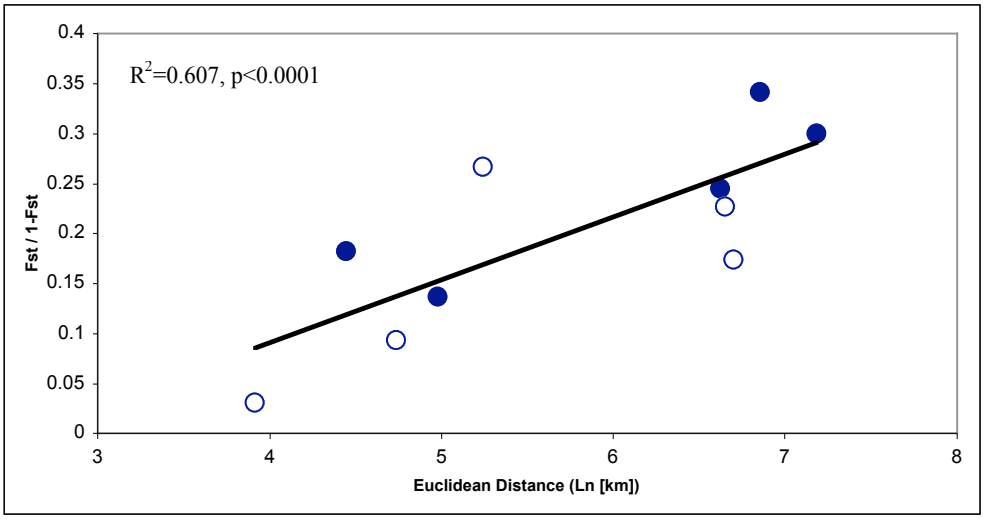

Figure 6b. Isolation by distance for groups (genetic populations) of *E. sezekorni*. Open circles represent island pairs included and filled circles represent island pairs excluded in the migration matrix. Regression line was fitted to all points.

M. waterhousii also showed significant IBD_{GEO} between islands (R^2=0.330, p<0.001, Figure 7). The slope of the IBD_{GEO} relationship was significantly lower for *M. waterhousii* (0.058, 95%CI 0.039-0.077) than for *E. sezekorni* at the island level (0.10, 95%CI 0.086-0.11) but not at the group level (0.081, 95%CI 0.039-0.12).

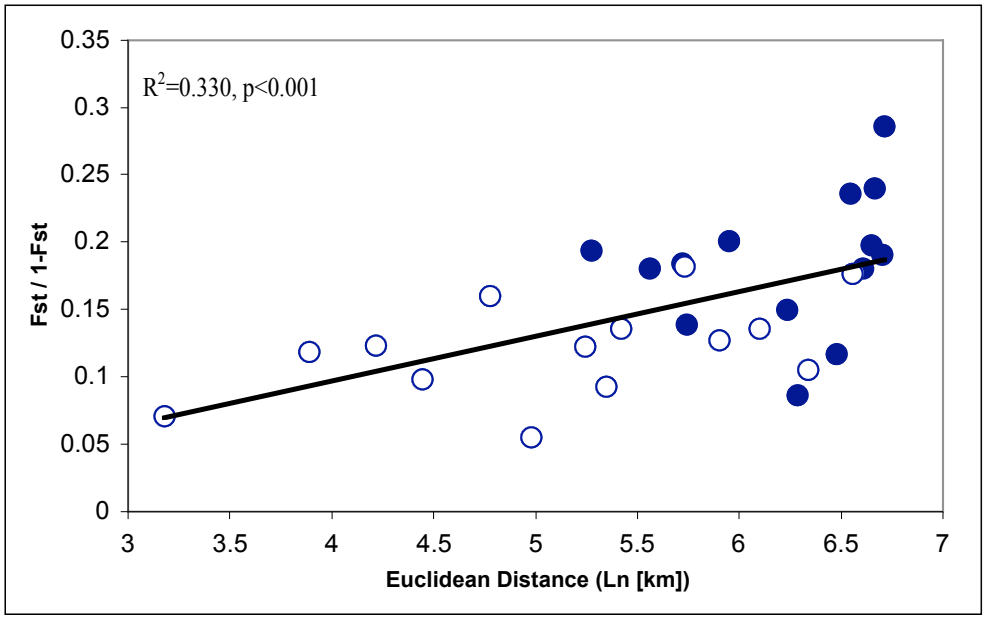

Figure 7. Isolation by distance for *M. waterhousii*. Open circles represent island pairs included and filled circles represent island pairs excluded in the migration matrix. Regression line was fitted to all points.

Effective distance was significantly correlated with genetic differentiation for *E. sezekorni* at the island level for both periods (*Annual* R^2=0.358, p=0.0001; *June* R^2=0.289, p=0.0001) but not at the group level for either time period (*Annual* R^2=0.174, p=0.22; *June* R^2=0.216, p=0.17) levels (Figure 8a-d). Effective distance was also significantly correlated with genetic differentiation in *M. waterhousii* for both periods (*Annual* R^2=0.205, p=0.01; *June* R^2=0.172, p=0.03) (Figure 9a,b). Overall, genetic differentiation was more strongly correlated with Euclidean distance than effective

distance in all cases. There were no significant relationships between the ratio of distance asymmetry and the ratio of migration asymmetry for either *E. sezekorni* or *M. waterhousii* based on either period of D_{WIND} values ($p>0.2$ for all cases) (data not shown). From these results, I conclude that both species displayed significant IBD_{GEO} and that IBD_{WIND} did not provide any additional explanatory power in predicting distribution of genetic diversity or instances of asymmetric gene flow.

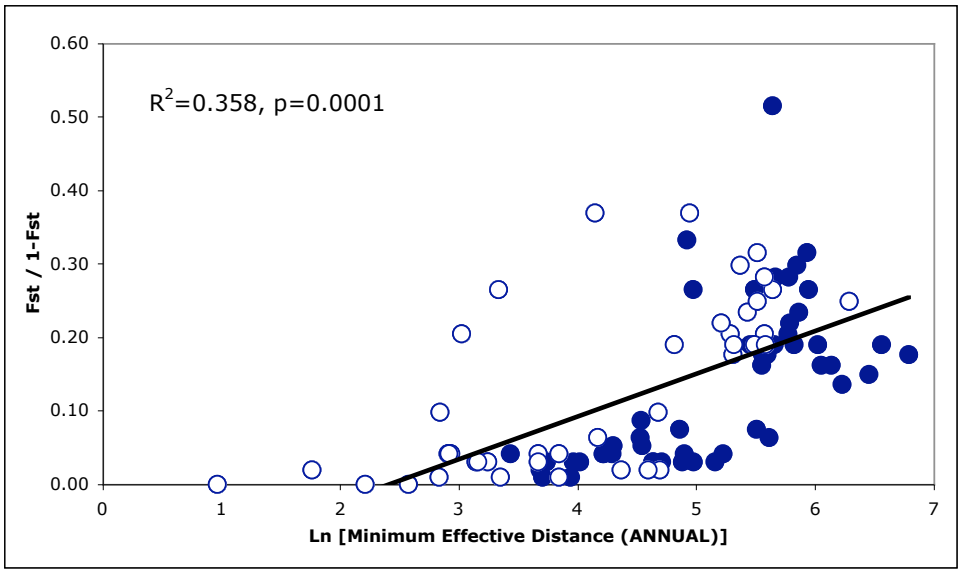

Figure 8a. Isolation by distance using minimum pairwise effective distance (minimum D_{ANNUAL}) for *E. sezekorni* at the island level. Open circles represent island pairs included and filled circles represent island pairs excluded in the migration matrix. Regression line was fit to all points.

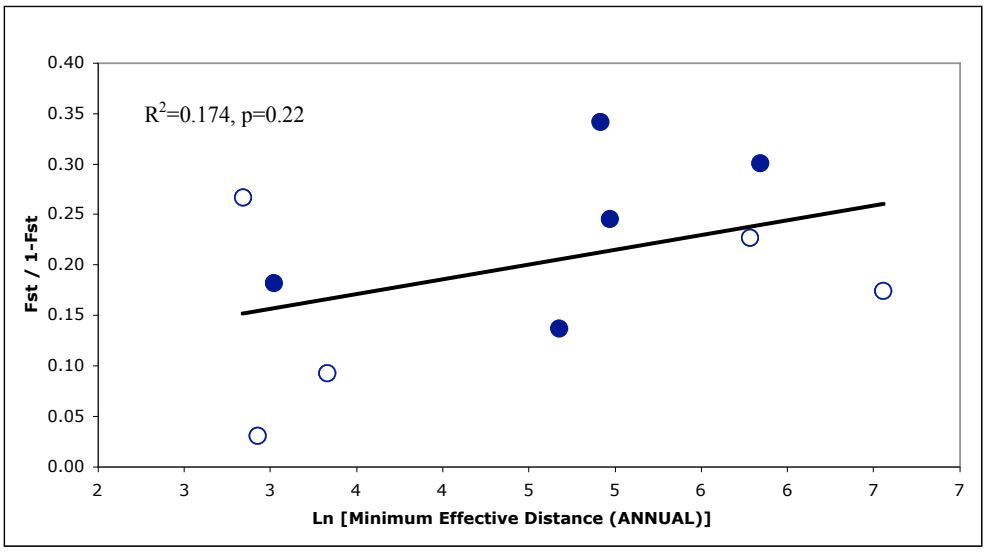

Figure 8b. Isolation by distance using minimum pairwise effective distance (minimum D_{ANNUAL}) for *E. sezekorni* at the group level. Open circles represent island pairs included and filled circles represent island pairs excluded in the migration matrix. Regression line was fitted to all points.

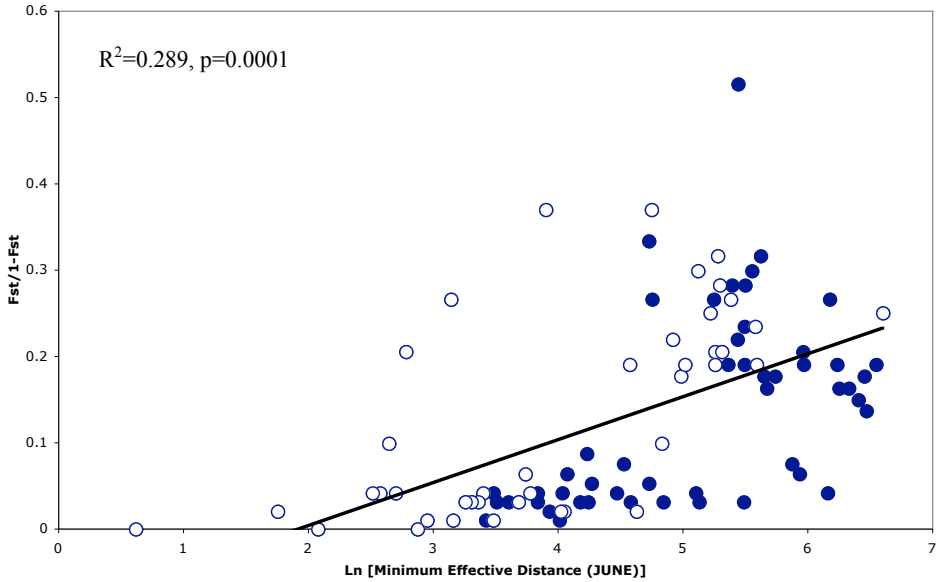

Figure 8c. Isolation by distance using minimum pairwise effective distance (minimum D_{JUNE}) for *E. sezekorni* at the island level. Open circles represent island pairs included and filled circles represent island pairs excluded in the migration matrix. Regression line was fitted to all points.

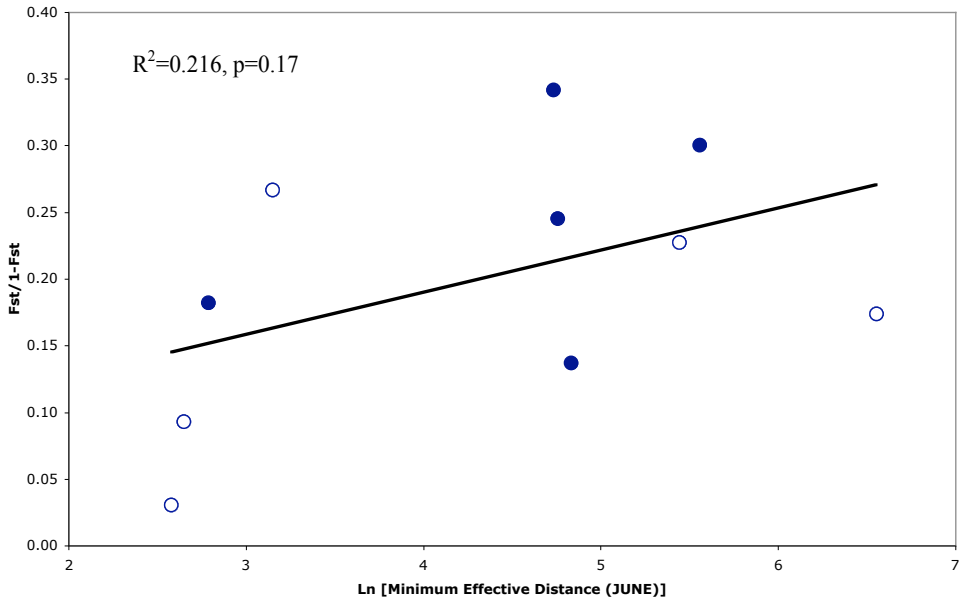

Figure 8d. Isolation by distance using minimum pairwise effective distance (minimum D_{JUNE}) for *E. sezekorni* at the group level. Open circles represent island pairs included and filled circles represent island pairs excluded in the migration matrix. Regression line was fitted to all points.

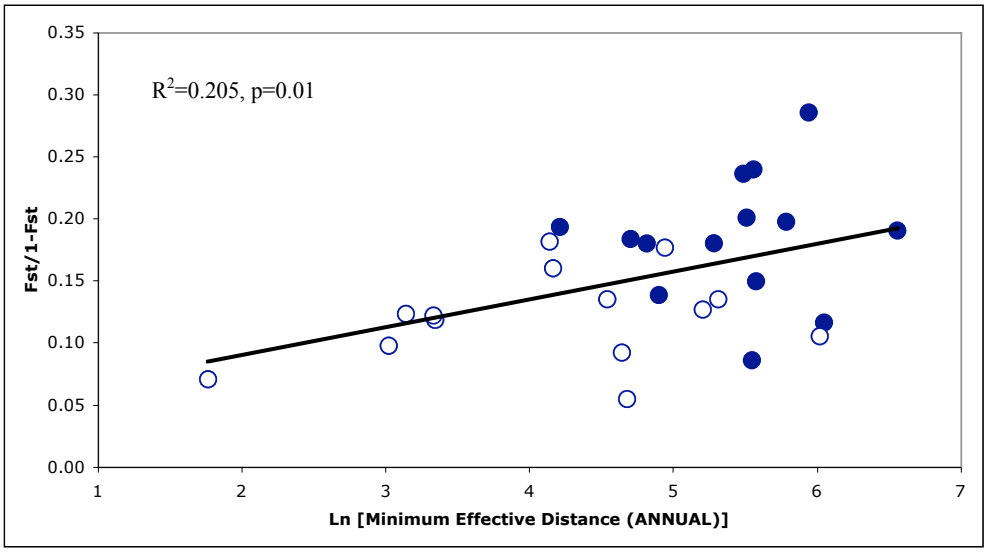

Figure 9a. Isolation by distance using minimum pairwise effective distance (minimum D_{ANNUAL}) for *M. waterhousii*. Open circles represent island pairs included and filled circles represent island pairs excluded in the migration matrix. Regression line was fitted to all points.

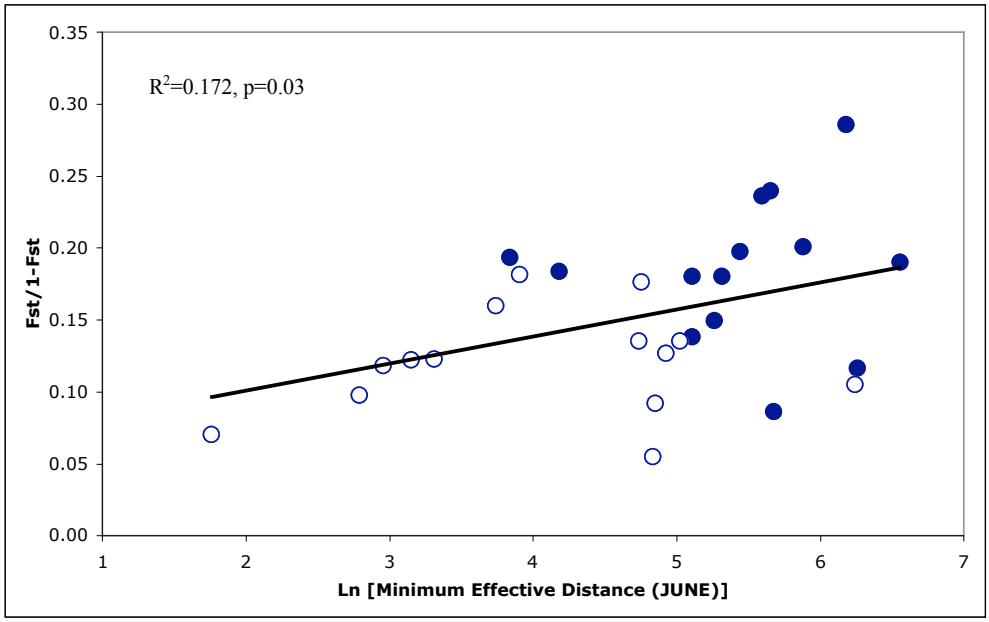

Figure 9b. Isolation by distance using minimum pairwise effective distance (minimum D_{JUNE}) for *M. waterhousii*. Open circles represent island pairs included and filled circles represent island pairs excluded in the migration matrix. Regression line was fitted to all points.

Chapter 4: Discussion

The results of this study reveal drastically different patterns of genetic structure in *E. sezekorni* and *M. waterhousii*. Concordant with the results of Fleming *et al.* (*in press*), island populations of *M. waterhousii* appear to be genetically isolated from one another. The strong genetic subdivisions between island populations of this species are indicative of a sedentary lifestyle and long residency time. Additional evidence for limited connectivity between island populations comes from this species' extinction pattern. Morgan (2001) reported that *M. waterhousii* has become extinct on six of the 30 islands (20%) from which it is included in the fossil record. These findings signify a geographical range contraction since the late Quaternary and suggest that recolonization events between islands are rare.

In contrast, *E. sezekorni* exhibits surprisingly less genetic structure than anticipated given its island endemism. I clearly detected a genetic separation between *E. sezekorni* bats on the eastern islands in its range (Hispaniola and Puerto Rico) versus the rest of the Greater Antilles and Bahamas. While consistent with both the current taxonomy of the genus (Simmons 2005) and the findings of Fleming *et al.* (*in press*), the division remains perplexing given the relatively short distance between Hispaniola and Cuba (85 km). Concordant results from STRUCTURE and MIGRATE analyses suggest greater westward gene flow from Puerto Rico to Hispaniola than vice versa (separated by 114 km). Despite a similar distance of separation, gene flow between Hispaniola and Cuba is very low in both directions. The 1700 m deep Windward Passage separating these two islands may represent the putative barrier that appears to have restricted gene flow in other West Indian bats (e.g. Natalidae; A. Tejedor *pers. comm*). Within the

eastern and western clades, however, genetic differentiation is low. In contrast to *M. waterhousii*, no populations have gone extinct on the 23 islands throughout the Greater Antilles and Bahamas where the genus occurs in the fossil record (Morgan 2001). Some inherent ecological difference such as dispersal ability between these two species thus appears to have produced very different genetic structure and susceptibility to extinction. Similarly, divergent patterns of genetic structure have been recorded among other phyllostomid species in the Lesser Antilles (e.g. *Ardops nichollsi*, *Brachyphylla cavernarum*, and *Artibeus jamaicensis*) (Carstens *et al.* 2004). The authors attributed the observed patterns to differential rates of gene flow among islands, incomplete lineage sorting, and ecological differences between these taxa.

The only significant departure from HW equilibrium in this study occurred at the island level in Puerto Rico for *E. sezekorni*. A potential explanation is the Wahlund effect, which refers to elevated levels of homozygosity when multiple distinct populations are erroneously treated as a single, interbreeding population (Freeland 2005). I reran STRUCTURE including only Puerto Rican samples to see if I could detect evidence for population substructure within Puerto Rico. The maximum log likelihood value occurred at K=1 (mean –711.6 +/- SD 2.09), however, suggesting inbreeding, not sample error, is responsible for the observed excess of homozygosity.

I detected asymmetric gene flow among a majority of pairwise population comparisons (80% in both species). One intuitive factor that may lead to asymmetric gene flow is unequal sizes of source populations. Under a neutral model, island size is correlated with a species' abundance, and larger islands should contribute a disproportionate number of migrants to smaller neighboring islands (Hubbell 1997). In

this study, however, island size did not explain directional bias of migration rates or estimated population sizes. In fact, effective population size in Jamaica was estimated to be significantly greater than the group or island with the second highest effective population size (by factors of 8 for *E. sezekorni* and 2 for *M. waterhousii*) despite being ranked third in area for both species (Tables 5 and 6). Sampling bias could lead to these results if sample size was greater on Jamaica than other islands (Beerli and Felsenstein 1999), but this was not the case. I am not currently able to explain these results, particularly because of the parallel pattern exhibited by both species.

Surface level trade winds were another intuitive candidate for generating asymmetric gene flow because of their effects on flight dynamics of volant organisms (Liechti 2006; Akesson and Hedenstrom 2007; Shamoun-Baranes *et al.* 2007). The results of this study, however, do not provide evidence that gene flow is mediated by wind for either of these species. In spite of these results, I cannot entirely rule out a potential mechanistic role of wind. Perhaps the limited spatial and temporal resolution of the wind data used in this study does not adequately capture the overall effect on the movement of bats between islands. The wind data did not include much variability at this broad spatial scale (see Figure 3). However, because the results from the MIGRATE analysis are best viewed as long-term parameter estimates (Hanfling and Weetman 2006), it seems appropriate to examine their relationship with long-term averages of wind. The central goal of this study was to see if instances of asymmetric gene flow could be attributed to the winds hypothetically encountered by a dispersing bat *on average*.

Another potential reason why wind may not mediate gene flow in these species is that their flight speeds are greater than the wind speeds they encounter during movements

between islands. While determining the specific effects of wind on the flight behavior of flying organisms is complex, the effect generally declines as the flight speed exceeds wind speed (Akesson and Hedenstrom 2007). Flight speed data do not currently exist for these species, but for comparative purposes, *Leptonycteris curasoae*, a strong flying phyllostomid, commutes between day roost and feeding areas at an average air speed of 8.2 m/s (Sahley *et al.* 1993), which is only slightly greater than the mean wind speeds recorded in my study area (see Figure 3a). Flight speeds of *E. sezekorni* and *M. waterhousii* are likely slower than those of *L. curasoae* (T. Fleming, *pers. comm.*), but perhaps the mean wind does not represent enough of an additional energetic cost to affect their movement patterns. In this case, maximum wind speed and direction, not mean values, may be more important in determining flight dynamics of these bats.

Among other factors that may account for the observed gene flow asymmetries, wind may still play a role in this system if anomalous events, such as hurricanes, contribute disproportionately to long distance dispersal of bats. Hurricanes have historically been a major climatological presence in the study area. According to Caviedes (1991), the Caribbean basin has experienced an average of three hurricane-strength events per year over the past 500 years. While it is feasible that these storms affect long distance dispersal of bats and other organisms in the region, the exact mechanism is difficult to resolve. Hurricanes can lead to a substantial decline in population sizes due to a combination of direct and indirect effects (i.e. decimated food supplies or destroyed roosting structures) (Jones *et al.* 2001; Gannon and Willig 1994). The stochastic nature of hurricanes, however, as well as species-specific responses to disturbance, makes the development of testable hypotheses about their effect on gene

flow all but impossible. There is anecdotal evidence of long distance dispersal of bats, including *E. sezekorni*, following hurricanes (T. Fleming, *pers. comm.*; Fleming *et al. unpubl. data*) but we do not know the exact mechanism leading to these 'transplants'. Interestingly, the annual peak in hurricane activity occurs in late summer, coinciding with the time when juvenile bats become volant and potentially dispersing from their natal colonies.

Given the broad spatial scale across which this study was conducted (D_{GEO} ranged from 3 – 1461 km), the significant difference in slope for the IBD relationship of the two species may provide some information about differences in their dispersal abilities. In a review of IBD of phytophagous insects, Peterson and Denno (1998) showed that dispersal ability influences the slope of IBD relationships. Across broad spatial scales, moderately mobile species exhibited a steeper IBD slope than both sedentary and highly mobile species (Peterson and Denno 1998). Widespread dispersal can lead to weak IBD because extensive gene flow among populations counteracts the effects of genetic drift and selection. The contrasting process in sedentary species that can lead to a parallel pattern is that gene flow is limited across the entire range of distances sampled and even nearby populations diverge genetically. It is possible that *M. waterhousii* would exhibit stronger IBD at a reduced spatial scale, perhaps among colonies within islands. Unfortunately, the sampling scheme of this study does not lend itself to a direct examination of this possibility. The relatively shallow IBD slope in *M. waterhousii*, however, along with its strong genetic differentiation among islands, provides strong support for limited over-water dispersal ability in this species. These results suggest that populations of *M. waterhousii* deserve greater taxonomic and conservation attention.

Literature Cited

Akesson, S. and Hedenstrom, A. 2007. How migrants get there: migratory performance and orientation. BioScience **57**: 123-133.

Anderson, S. 1969. *Macrotus waterhousii*. Mammalian Species **1**: 1-4.

Baker, R. J. and H. H. Genoways. 1978. Zoogeography of Antillean bats. Pages 53-97 *in* F.B. Gill, editor. Zoogeography in the Caribbean. Academy of Natural Sciences of Philadelphia, Philadelphia.

Baker, R. J., S. R. Hoofer, C. A. Porter, and R. A. Van den Bussche. 2003. Diversification among New World leaf-nosed bats: an evolutionary hypothsis and classification inferred from digenomic congruence of DNA sequences. Occasional Papers, Museum of Texas Tech University **230**: 1-32.

Beerli, P. 2004. MIGRATE: documentation and program, part of LAMARC. Version 2.0. Revised December 23, 2004. Distributed over the internet, http://evolution.gs.washington.edu/lamarc.html [Downloaded: April 2005].

Beerli, P. and J. Felsenstein. 2001. Maximum likelihood estimation of a migration matrix and effective population sizes in n subpopulations by using a coalescent approach. PNAS 98(8): 4563-4568.

Calsbeek, R. and T. B. Smith. Ocean currents mediate evolution in island lizards. 2003. Nature **426**: 552-555.

Caviedes, C. N. 1991. Five hundred years of hurricanes in the Caribbean: Their relationship with global climatic variables. GeoJournal **23**: 301-310.

Clark Labs, Clark University. 2006. Idrisi Andes Version 15. 950 Main Street, Worcester, MA, USA.

Cook, L. G. and M. D. Crisp. 2005. Directional asymmetry of long-distance dispersal and colonization could mislead reconstructions of biogeography. Journal of Biogeography **32**: 741-754.

Coulon, A., J. F. Cosson, J. M. Angibault, B. Cargnelutti, M. Galan, N. Morellet, E. Petit, S. Aulagnier and A. J. M. Hewison. 2004. Landscape connectivity influences gene flow in a roe deer population inhabiting a fragmented landscape: an individual-based approach. Molecular Ecology **13**: 2841-2850.

Cushman, S. A., K. S. McKelvey, J. Hayden and M. K. Schwartz. 2006. Gene flow in complex landscapes: testing multiple hypotheses with causal modeling. The American Naturalist **168**: 486-499.

Davalos, L. M. 2004. Phylogeny and biogeography of Caribbean mammals. Biologica4l Journal of the Linnean Soceity **81**: 373-394.

Dias, P. C. 1996. Sources and sinks in population biology. Trends in Ecology and Evolution **11**: 327-330.

Dutech, C., V. L. Sork, A. J. Irwin, P. E. Smouse and F. W. Davis. 2005. Gene flow and fine-scale genetic structure in a wind-pollinated tree species, *Quercus lobata* (Fagaceaee). American Journal of Botany **92**: 252-261.

ESRI, Inc. 2002. ArcView GIS 3.3. 380 New York Street, Redlands, CA, USA.

Excoffier, L., G. Laval and S. Schneider. 2005. Arlequin ver. 3.0: An integrated software package for population genetics data analysis. Evolutionary Bioinformatics Online **1**: 47-50.

Fleming, T. H., K. L. Murray and B. Carstens. *in press*. Phylogeography and genetic structure of three evolutionary lineages of West Indian phyllostomid bats. Chapter 5 *in* Evolution, Ecology, and Conservation of Island Bats (T.H. Fleming and P.A. Racey, eds.). Chicago, IL: University of Chicago Press.

Fraser, D. J., C. Lippe and L. Bernatchez. 2004. Consequences of unequal population size, asymmetric gene flow and sex-biased dispersal on population structure in brook charr (*Salvelinus fontinalis*). Molecular Ecology **13**: 67-80.

Freeland, J. R. 2005. Molecular Ecology. John Wiley & Sons Ltd. pp388. West Sussex, England.

Funk, W. C., M. S. Blouin, P.S. Corn, B.A. Maxell, D.S. Pilloid, S. Amish and F.W. Allendorf. 2005. Population structure of Columbia spotted frogs (*Rana luteiventris*) is strongly affected by the landscape. Molecular Ecology **14**: 483-496.

Galindo, H. M., Olson, D. B. and S. R. Palumbi. 2006. Seascape genetics: a coupled oceanographic-genetic model predicts population structure of Caribbean corals. Current Biology **16**: 1622-1626.

Genoways, H. H., R. J. Baker, J. W. Bickham and C. J. Phillips. 2005. Bats of Jamaica. Special Publications of the Museum, Texas Tech University **48**: 1-155.

Goudet, J., N. Perrin and P. Waser. 2002. Tests for sex-biased dispersal using bi-parentally inherited genetic markers. Molecular Ecology **11**: 1103-1114.

Goudet, J. 2001. FSTAT, a program to estimate and test gene diversities and fixation indices (version 2.9.3). Available from http://www.unil.ch/izea/softwares/fstat.html.

Hanfling, B. and D. Weetman. 2006. Concordant genetic estimators of migration reveal anthropogenically enhanced source-sink population structure in the River Sculpin, *Cottus gobio*. Genetics **173**: 1487-1501.

Hanski, I. 1999. *Metapopulation Ecology*. Oxford, UK: Oxford University Press.

Hare, M. P., C. Guenther and W. F. Fagan. 2005. Nonrandom larval dispersal can steepen marine clines. Evolution **59**: 2509-2517.

Jenness, J. 2004. Distance and bearing between matched features (distbyid.avx) extension for ArcView 3.x, v. 2. Jenness Enterprises. Available at: http://www.jennessent.com/arcview/distance_by_id.htm.

Jensen, J., A. J. Bohonak and S. K. Kelley. 2005. Isolation by Distance Web Service. BMC Genetics 6: 13.

Jones, K. E. O. R. P. bininda-Emonds and J. L. Gittleman. 2005. Bats, clocks, and rocks: diversification patterns in Chiroptera. Evolution **59**: 2243-2255.

Kawecki, T. J. and R. D. Holt. 2002. Evolutionary consequences of asymmetric dispersal rates. The American Naturalist **160**: 333-347.

Kennington, W. J., J. Gockel and L. Partridge. 2003. Testing for asymmetrical gene flow in a *Drosophila melanogaster* body-size cline. Genetics **165**: 667-673.

Kirkpatrick, M. and N. H. Barton. 1997. Evolution of a species' range. American Naturalist **150**: 1-23.

Koopman, K. F. 1993. Order Chiroptera. Pages 137-241 *in* D. E. Wilson and D. M. Reeder, editors. Mammal species of the world. Smithsonian Institution Press, Washington, DC.

Liechti, F. 2006. Birds: blowin' by the wind? Journal of Ornithology **147**: 202-211.

Mantel, N. 1967. The detection of disease clustering and a generalized regression approach. Cancer Research **27**: 209-220.

Manel, S., M. K. Schwartz, G. Luikart and P. Taberlet. 2003. Landscape genetics: combining landscape ecology and population genetics. Trends in Ecology and Evolution **18**: 189-197.

Michels, E., K. Cottenie, L. Neys, K. De Gelas, P. Coppin and L. De Meester. 2001. Geographical and genetic distances among zooplankton populations in a set of interconnected ponds: a plea for using GIS modelling of the effective geographical distance. Molecular Ecology **10**: 1929-1938.

Morgan, G. S. 2001. Patterns of extinction in West Indian bats. Pages 368-407 *in* C. A. Woods and F. E. Sergile, editors. Biogeography of the West Indies: patterns and perspectives. CRC Press, Boca Raton, FL.

Munoz, J., A. M. Felicisimo, F. Cabezas, A. R. Burgaz and I. Martinez. 2004. Wind as a long-distance dispersal vehicle in the southern hemisphere. Science **304**: 1144-1147.

Nowak, R. M. 1994. Walker's bats of the world. The Johns Hopkins University Press, Baltimore, MD. 288 pp.

Peterson, M. A. and R. F. Denno. 1998. The influence of dispersal and diet breadth on patterns of genetic isolation by distance in phytophagous insects. The American Naturalist **152**: 428-446.

Pritchard, J. K., M. Stephens, and P. Donnelly. 2000. Inference of population structure using multilocus genotype data. Genetics **155**: 945–959.

Renner, S. 2004. Plant dispersal across the tropical Atlantic by wind and sea currents. International Journal of Plant Sciences **165**: S23-S33.

Rodriguez-Duran, A. 1995. Metabolic rates and themal conductance in four species of neotropical bats roosting in hot caves. Comparative Biochemistry and Physiology **110A**: 347-355.

Rousset, F. 1997. Genetic differentiation and estimation of gene flow from *F*-statistics under isolation by distance. Genetics **145**: 1219-1228.

Sahley, C. T., M. A. Horner, T. H. Fleming. 1993. Flight speeds and mechanical power outputs of the nectar-feeding bat, *Leptonycteris curasoae* (Phyllostomidae, Glossophaginae). Journal of Mammalogy **74**: 594-600.

Shamoun-Baranes, J. E. van Loon and F. Liechti. 2007. Analyzing the effect of wind on flight: pitfalls and solutions. Journal of Experimental Biology **210**: 82-90.

Silva Taboada, G. 1979. Los Murcielagos de Cuba. Editora de la Academia de Ciencias de Cuba, Havana.

Simmons, N. B. 2005. Order Chiroptera. Pages 312-529 *in* D. E. Wilson and D. M. Reeder, editors. Mammal species of the world, a taxonomic and geographic reference. Johns Hopkins Press, Baltimore, Maryland.

Slatkin, M. 1987. Gene flow and the geographic structure of natural populations. Science, New Series **236**: 787-792.

Spear, S. S., C. R. Peterson, M. D. Matocq and A. Storfer. 2005. Landscape genetics of the blotched tiger salamander (*Ambystoma tigrinum melanostictum*). Molecular Ecology **14**: 2553-2564.

Stevens, V. M., C. Verkenne, S. Vandewoestijne, R. A. Wesselingh and M. Baguette. 2006. Gene flow and functional connectivity in the natterjack toad. Molecular Ecology **15**: 2333-2344.

Teeling, E. C., M. S. Springer, O. Madsen, P. Bates, S. J. O'Brien and W. J. Murphy. 2005. A molecular phylogeny for bats illuminates biogeography and the fossil record. Science **307**: 580-584.

Telschow, A., J. Engelstadter and N. Ymamura. 2006. Asymmetric gene flow and constraints on adaptation caused by sex ratio distorters. Journal of Evolutionary Biology **19**: 869-878.

Thompson, J. N. 1994. The Coevolutionary Process. The University of Chicago Press, Chicago.

Wares, J. P., S. D. Gaines and C. W. Cunningham. 2001. A comparative study of asymmetric migration events across a marine biogeographic boundary. Evolution **55**: 295-306.

Whitlock, M. C. and D. E. McCauley. 1999. Indirect measures of gene flow and migration: Fst≠1/(4*Nm*+1). Heredity **82**: 117-125.

Wright, S. 1946. Isolation by distance under diverse systems of mating. Genetics **31**: 39-59.

Vignieri, S. N. 2005. Streams over mountains: influence of riparian connectivity on gene flow in the Pacific jumping mouse (*Zapus trinotatus*). Molecular Ecology **14**: 1925-1937.

Vuilleumier, S. and H. P. Possingham. 2006. Does colonization asymmetry matter in metapopulations? Proceedings of the Royal Society B **273**: 1637-1642.